

DBL-1/TGF- $\beta$  SIGNALING IN *C. ELEGANS*: TRAFFICKING AND RESPONSES

A THESIS

SUBMITTED IN PARTIAL FULFILLMENT OF THE REQUIREMENTS  
FOR THE DEGREE OF MASTER OF SCIENCE  
IN THE GRADUATE SCHOOL OF THE  
TEXAS WOMAN'S UNIVERSITY

DEPARTMENT OF BIOLOGY  
COLLEGE OF ARTS AND SCIENCES

BY  
GEETHANJALI RAVINDRANATHAN

DENTON, TEXAS

MAY 2018

Copyright © 2018 by Geethanjali Ravindranathan

## DEDICATION

*To my Grandma*

## ACKNOWLEDGEMENTS

I thank Dr. Gumienny for her mentorship and guidance towards my professional and personal growth. I am grateful to the Gumienny lab for their constant support and assistance. I am thankful for all the resources that helped me successfully conduct my research. I thank all my committee members for their valuable guidance, encouragement, and direction. I am grateful to all the faculty and staff who have helped me in my journey. I thank the Biology Department and all the funding agencies that provided scholarships to me through the department. I also thank the National Institutes of Health (R01GM097591) for supporting my research. It is especially an honor to be a Virginia Chandler Dykes Scholar in my time at Texas Woman's University. I thank TWU for providing innumerable opportunities for growth and development. I thank my family for their love and support across oceans. I thank my friends who have cared for me like family and made my days brighter. Lastly, I am grateful to everything that inspires me to keep growing in life.

## ABSTRACT

GEETHANJALI RAVINDRANATHAN

DBL-1/TGF- $\beta$  SIGNALING IN *C. ELEGANS*: TRAFFICKING AND RESPONSES

MAY 2018

*Introduction:* Transforming growth factor-beta (TGF- $\beta$ ) comprises a conserved family of secreted cell signaling proteins responsible for regulating numerous cellular processes. In the nematode *Caenorhabditis elegans*, one TGF- $\beta$  is DBL-1. Secretion of TGF- $\beta$  from sending cells is a process that is not well understood for any TGF- $\beta$ . It is also unclear how TGF- $\beta$  signaling plays a role in organismal responses to various external factors. *Methods:* First, we characterized DBL-1 trafficking and responses. Second, we determined how the nematode surface barrier is affected by DBL-1 signaling. Third, we analyzed toxicity of three nanocarrier and two potential anti-cancer compounds to *C. elegans*. *Results & Conclusions:* We discovered UNC-108 and CAV-1 are involved in trafficking DBL-1. Next, we identified changes in surface barrier, which can be exploited for anthelmintic therapy. Lastly, we established the lack of toxicity of five compounds to *C. elegans*, which supports their further testing in higher organisms.

## TABLE OF CONTENTS

	Page
DEDICATION .....	ii
ACKNOWLEDGEMENTS .....	iii
ABSTRACT .....	iv
LIST OF TABLES .....	viii
LIST OF FIGURES .....	ix
LIST OF ABBREVIATIONS .....	x
 Chapter	
I. INTRODUCTION .....	1
The TGF- $\beta$ superfamily signaling pathway .....	1
<i>C. elegans</i> TGF- $\beta$ signaling .....	3
Advantages of the <i>C. elegans</i> model system.....	7
Using <i>C. elegans</i> to test compounds for toxicity .....	10
Conclusions .....	12
II. DBL-1 TRAFFICKING AND ITS ROLE IN CHANGING THE SURFACE	
BARRIER OF <i>C. ELEGANS</i> .....	13
Introduction .....	13
Materials and Methods .....	17
Strains and maintenance .....	17
Microscopy analysis .....	18
<i>dbl-1</i> expression analysis.....	18

Colocalization Studies .....	19
Worm-star formation assays .....	19
Surface barrier analysis .....	20
Results .....	20
DBL-1 localizes to cholinergic ventral cord neurons of <i>C. elegans</i> .....	20
UNC-108/Rab GTPase and DBL-1/TGF- $\beta$ colocalize.....	22
CAV-1/caveolin and DBL-1/TGF- $\beta$ colocalize .....	23
BEC-1/beclin1 autophagy-related protein and DBL-1/TGF- $\beta$ do not colocalize.....	24
<i>dbl-1</i> /TGF- $\beta$ strains form worm-stars and lipid composition of their surface barrier is different from wild-type .....	25
Discussion .....	27
III. ROLE OF <i>C. ELEGANS</i> DBL-1 IN GENERATING AN ORGANISMAL STRESS	
RESPONSE TO TEST COMPOUNDS.....	31
Introduction .....	31
Materials and Methods .....	35
Strains and maintenance .....	35
Test compounds and controls .....	35
Compound intake.....	36
Chemotaxis assay .....	37
Locomotion assay .....	37
Body length assay .....	38
Survival assay .....	39
Results .....	39
Fluorescent test compounds are ingested by <i>C. elegans</i> .....	39
Test compounds exhibit a positive chemotaxis to the compounds.....	41
Test compounds do not affect motility .....	42
Test compounds do not affect body length.....	43
Test compounds do not affect survival.....	44
Discussion .....	47

IV. CONCLUSIONS AND FUTURE DIRECTIONS .....	50
V. REFERENCES.....	54
APPENDIX	
A. ELUCIDATING THE ROLE OF INSULIN SIGNALING IN DYF-7 RESPONSES IN <i>C. ELEGANS</i> .....	69

## LIST OF TABLES

Table	Page
2.1. TGF- $\beta$ superfamily signaling is conserved in eukaryotes. ....	15
2.2. Genes studied, their homologs, and their major known functions.....	16
2.3. Expression of DBL-1 in ventral nerve cord (VNC) cells with reference figure of the VNC cells.....	2
2.4. Worm-star formation occurs in DBL-1 pathway mutants. ....	26
3.1. Test compounds do not alter body length of animals. ....	44



## LIST OF FIGURES

Figure	Page
1.1. TGF- $\beta$ /DBL-1 signaling pathway in <i>C. elegans</i> .....	5
2.1. Canonical and non-canonical TGF- $\beta$ /DBL-1 signaling pathway in <i>C. elegans</i> . ....	14
2.2. TEM micrographs of differences in amount of lipids in <i>C. elegans</i> strains .....	17
2.3. Colocalization of UNC-108 and DBL-1.....	23
2.4. Colocalization of CAV-1 and DBL-1.....	24
2.5. Colocalization of BEC-1 and DBL-1.....	25
2.6. Representative GC-FID chromatograms of surface lipids.....	27
3.1. Fluorescent compounds are ingested but not degraded in <i>C. elegans</i> . ....	40
3.2. <i>C. elegans</i> strains tested exhibit positive chemotaxis to test compounds.....	2
3.3. Test compounds do not affect locomotion of animals. ....	43
3.4. Survival of animals was not affected by test compounds. ....	45
4.1. Model TGF- $\beta$ /DBL-1 trafficking in <i>C. elegans</i> .....	50
A.1. DAF-2 and DAF-16 do not affect DYF-7 function. ....	72

## LIST OF ABBREVIATIONS

ANOVA	Analysis of variance
ATP	Adenosine triphosphate
BEC-1	Beclin ortholog in <i>C. elegans</i>
BMP	Bone morphogenetic protein
CAN	Canal associated neuron
CAV-1	Caveolin ortholog in <i>C. elegans</i>
CGC	<i>Caenorhabditis</i> Genetics Center
CPD	Cyclobutanepyrimidine dimers
DAF-16	Forkhead box O homolog in <i>C. elegans</i>
DAF-4	Type II TGF- $\beta$ receptor ortholog in <i>C. elegans</i>
DAF-2	Insulin/IGF receptor ortholog in <i>C. elegans</i>
DBL-1	TGF- $\beta$ ligand in <i>C. elegans</i>
DMSO	Dimethylsulfoxide
DNA	Deoxyribonucleic acid

DRAG-1	GPI-anchor protein of the repulsive guidance molecule family
dsRNA	Double stranded RNA
DYF-7	Tectorin-like ZP-domain protein in <i>C. elegans</i>
EMS	Ethyl methane sulfonate
FID	Flame ionization detector
FOXO	Forkhead box O
FUDR	5-fluoro-2'-deoxyuridine-5'-phosphate
GABA	Gamma-Aminobutyric acid
GC	Gas chromatography
GFP	Green fluorescent protein
HAT	Histone acetyl transferase
HDAC	Histone deacetylase
L1	Larval stage 1 of <i>C. elegans</i>
L2	Larval stage 2 of <i>C. elegans</i>
L3	Larval stage 3 of <i>C. elegans</i>
L4	Larval stage 4 of <i>C. elegans</i>

LD50	Lethal dose killing 50% of test sample
LON-2	Member of the glypican family of heparan sulfate proteoglycans
LRIG	Leucine rich repeats and immunoglobulin-like domains
mRFP	Monomeric red fluorescent protein
MS	Mass spectrometry
N2	Wild type <i>C. elegans</i> strain
NGM	Nematode growth media
PCC	Pearson's correlation coefficient
RGM	Repulsive guidance molecule
RNA	Ribonucleic acid
RNAi	RNA interference
SD	Standard deviation
SEM	Standard error of means
SMA-2	SMAD-2 regulatory SMAD ortholog in <i>C. elegans</i>
SMA-3	SMAD-2 regulatory SMAD ortholog in <i>C. elegans</i>
SMA-4	SMAD-2 co-mediator SMAD ortholog in <i>C. elegans</i>

SMA-6	Type I TGF- $\beta$ receptor ortholog in <i>C. elegans</i>
TEM	Transmission electron microscopy
TGF- $\beta$	Transforming growth factor beta
UNC-108	RAB-2 small GTPase ortholog in <i>C. elegans</i>
UV	Ultraviolet radiation
VNC	Ventral nerve cord

## CHAPTER I

### INTRODUCTION

#### The TGF- $\beta$ superfamily signaling pathway

The work presented in this thesis expands our understanding of an ancient cell signaling pathway, which is defined by the transforming growth factor  $\beta$  (TGF- $\beta$ ) superfamily of ligands (Feng and Derynck 2005). These cell signaling molecules are involved in regulating numerous cellular processes during embryogenesis as well as in mature tissues in organisms from nematodes and flies to mammals, including stress responses, proliferation, and determination of developmental fate (Wu and Hill 2009). Mutations in the genes for TGF- $\beta$ , its receptors, or intracellular signaling molecules associated with TGF- $\beta$  lead to developmental defects and diseases, such as vascular defects, bone abnormalities, and cancers (Blobe *et al.* 2000; Padua and Massague 2009; Wu and Hill 2009; Meulmeester and Ten Dijke 2011). Imbalances in the regulation of TGF- $\beta$  have been linked to numerous disease states such as atherosclerosis and fibrotic disease of the kidney, liver, and lung (Blobe *et al.* 2000).

The large TGF- $\beta$  superfamily divides into two subfamilies based on structural and functional relatedness: the TGF- $\beta$  isoforms, Nodal and Activins, and the bone morphogenetic proteins (BMPs) and growth differentiation factors (GDFs). The TGF- $\beta$  superfamily comprises more than 30 genes in mammals, 7 genes in *Drosophila*, and 5 genes in *C. elegans*. The ligands are expressed and secreted into the extracellular matrix

(ECM) as pre-proteins. Dimerization and stabilization require the pro-domain and the mature ligands are cleaved from the prodomain by furin-like convertase before they are secreted (Shi *et al.* 2011). At the extracellular surface of the receiving cell, an active TGF- $\beta$  ligand dimer brings together two pairs of transmembrane receptor serine/threonine kinases known as type II and type I receptors. Compared to the large number of TGF- $\beta$  ligands, there are only five type II receptors (T $\beta$ RII) and seven type I receptors (T $\beta$ RI) identified in humans (Poniatowski Ł *et al.* 2015). TGF- $\beta$  ligand binding stabilizes the interaction of the T $\beta$ RII dimer with two T $\beta$ RI molecules, forming heterotetrameric, active receptor complexes (Feng and Derynck 2005). Ligand-bound high affinity type II receptor recruits type I receptor and this process is facilitated by direct interaction between type II and type I receptor (Groppe *et al.* 2008). Ligand binding and receptor complex formation causes the cytoplasmic kinase domain of type II receptor to phosphorylate the GS domain on type I receptor, which in turn activates type I receptor kinase activity.

Upon binding TGF- $\beta$ s, type II receptor phosphorylates and activates type I receptor. The intracellular signal transducers (R-Smads) then are phosphorylated by type I receptor, and in turn, form complexes with Co-Smad (Chen *et al.* 1998). Smads exist in three subgroups: (1) receptor-regulated Smads (R-Smads; e.g. Smad1, 2, 3, 5, and 8 in vertebrates, Mad in *Drosophila*, SMA-2 and -3, and DAF-8 and -14 in *C. elegans*); (2) common Smads (Co-Smads; e.g. Smad4 in vertebrates, SMA-4, and DAF-3 in *C. elegans*); (3) inhibitory Smads (I-Smads; e.g. Smad6 and 7 in vertebrates and Dad in *Drosophila*). Those Smad complexes accumulate in the nucleus, and with the help of

other transcriptional cofactors, modulate transcription of target genes. Mammalian TGF- $\beta$  and activins signal their transcription responses through Smad2 and Smad3, whereas BMPs signal through Smad1, Smad5 and Smad8 (Mangahas 2008).

The founding member of the Smad family is the product of the *Drosophila* gene Mad (mothers against dpp), followed by three Mad homologues identified in *C. elegans*, called *sma-2*, *sma-3*, and *sma-4* (Sekelsky *et al.* 1995; Savage *et al.* 1996). Many homologs were later discovered in vertebrates and named Smad (as a merge of MAD and SMA). R-Smads and Co-Smads contains highly conserved MH1 (N-terminal) and MH2 (C-terminal) domains linked by a more diverse linker region. The MH1 domain has approximately 130 amino acids and contributes to the DNA-binding activity. R-Smads can directly interact with type I receptor through the MH2 domain and have a C-terminal SSXS motif, in which the last two serines are direct targets for phosphorylation by type I receptor (Souchelnytskyi *et al.* 1997). Phosphorylation of the SSXS motif in R-Smads leads to a conformational change, resulting in dissociation of R-Smad from type I receptor and formation of a trimeric Smad complex consisting of two R-Smads and a Co-Smad. This trimeric Smad complex then accumulates in the nucleus and regulates gene expression, positively or negatively, usually in association with other transcriptional cofactors (Derynck and Zhang 2003; Shi and Massague 2003; Feng and Derynck 2005; Moustakas and Heldin 2009b).

#### *C. elegans* TGF- $\beta$ signaling

In *C. elegans*, five TGF- $\beta$  ligands with non-redundant, non-lethal functions that share at least 70% sequence homology with human superfamily members have been



identified: DAF-7, DBL-1, UNC-129, TIG-2, and TIG-3. DAF-7 is a TGF- $\beta$ -related ligand and DBL-1 is more related to mammalian BMP2 and BMP4 and *Drosophila* Dpp. Their downstream signaling components have also been characterized, referred to as the Dauer pathway and the Sma/Mab pathway, respectively (Suzuki *et al.* 1999; Gumienny and Savage-Dunn 2013a). The Sma/Mab pathway was first shown to regulate body size and the development of male-specific sensory rays and copulatory spicules (Savage *et al.* 1996). Mutants of components in this pathway have small body size (Sma) phenotype and abnormal male tail (Mab) phenotype. DBL-1 acts as a dose-dependent regulator of body size; *dbl-1* overexpression results in longer animals (Morita *et al.* 1999b; Schultz *et al.* 2014). DBL-1 acts as the ligand and SMA-6 is the type I receptor (see Figure 1.1) (Krishna *et al.* 1999; Suzuki *et al.* 1999). The type II receptor DAF-4 is shared with the DAF-7 dauer pathway. *dbl-1* pathway mutants show decreased seam cell length but normal seam cell nuclei number, suggesting that decreases in cell size rather than cell number are responsible for the *dbl-1* Sma phenotype (Wang *et al.* 2002). Organ size measurements have shown that different organs are reduced in size to different degrees. The body length phenotype is known to develop during postembryonic development, and is not dependent on cell number, as this eutelic nematode species has a fixed somatic cell number among its members (Suzuki *et al.* 1999; Flemming *et al.* 2000; Nagamatsu and Ohshima 2004).

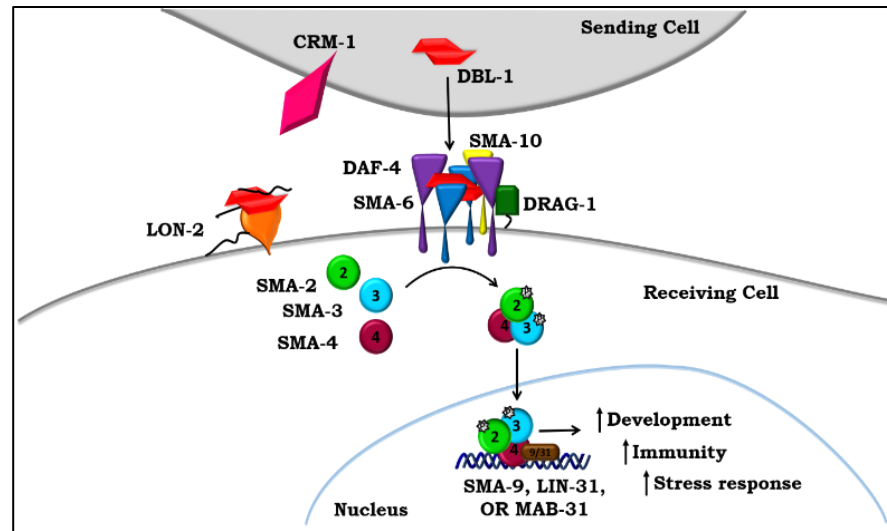


Figure 1.1. TGF- $\beta$ /DBL-1 signaling pathway in *C. elegans*. TGF- $\beta$ /DBL-1 promotes body size, male tail morphogenesis, cell lineage decisions, and innate immune responses. The DBL-1 signal (red) is secreted and received by a heterotetrameric receptor composed of two SMA-6 type I receptor and two DAF-4 type II receptor subunits (blue and purple, respectively). Extracellular regulators of DBL-1 signaling include CRM-1 (pink), which acts at the sending cell membrane or in the extracellular space to promote DBL-1 signaling, SMA-10 and DRAG-1 (yellow and green, respectively), which promote DBL-1 signaling at the membrane of the receiving cell, and LON-2/glypican (orange), which inhibits DBL-1 signaling at the receiving cell. The DBL-1 signal is transduced by SMA-2, SMA-3, and SMA-4 Smads. Transcription factors (browns) that act with Smads to carry out DBL-1-mediated responses include SMA-9/Schnurri, LIN-31/forkhead, and MAB-31. Image adapted from Gumienny and Savage-Dunn (2013).

The hypodermis is an epidermal tissue that surrounds the animal's internal tissues and synthesizes the nematode cuticle, a protective extracellular matrix (Yoshida *et al.* 2001; Wang *et al.* 2002; Schulenburg *et al.* 2004). The DBL-1 receptors, Smads, other regulatory factors, and a multitude of pathway targets are known to be expressed in the hypodermis. Loss of single cuticular proteins can also alter nematode body length (Brenner 1974; Page and Johnstone 2007; Fernando *et al.* 2011).

In addition to the Sma phenotype, a Mab phenotype is also found in these mutants. Male tail sensory rays and spicules are essential for mating. Normally in wild

type animals, there are nine rays on each side of the male tail. However, *dbl-1*, *daf-4*, *sma-2*, *sma-3*, *sma-4*, and *sma-6* mutant males show abnormal ray fusions and crumpled spicules. Ray fusion frequently occurs between rays 4-5, 6-7, and 8-9 (Savage *et al.* 1996).

In addition to body size regulation and male tail development, the Sma/Mab pathway has been shown to regulate innate immunity of *C. elegans*. The genes, *sma-2*, *sma-3*, *sma-4* and *sma-6* are required for resistance to *Pseudomonas aeruginosa* infection. The loss-of-function mutants of those four genes are hypersensitive to infection (Mallo *et al.* 2002). DBL-1 pathway regulators have been found that act on secreted DBL-1 or its receptors. It has been shown that LON-2 can negatively regulate Sma/Mab pathway activity. Hypodermally expressed LON-2 is a conserved member of the glypican family of heparan sulfate proteoglycans that can bind BMP2 *in vitro* (Gumienny *et al.* 2007). *lon-2(lf)* mutations result in a long body size phenotype and the *Drosophila* glypican gene *dally* rescues the *lon-2(lf)* body size defect (Gumienny *et al.* 2007). The sole member of the repulsive guidance molecule (RGM) family of proteins in *C. elegans*, DRAG-1, and member of a family with leucine rich repeats and immunoglobulin-like domains (LRIG), SMA-10 are found to positively regulate Sma/Mab pathway activity at the ligand-receptor level (Gumienny *et al.* 2010; Tian *et al.* 2010).

Despite all the groundbreaking studies at the level of the receiving cell, we still do not have a full understanding of how TGF- $\beta$  signals are trafficked and regulated by secreting cells and between sending and receiving cells. Specifically, how secreting cells determine and control how much TGF- $\beta$  to secrete and identifying all the players

controlling TGF- $\beta$  bioavailability between secretion and receptor activation. In our study, we used *C. elegans* to identify novel regulators of trafficking TGF- $\beta$  in the signaling pathway that act within the secreting cell (Chapter II).

Loss of signaling by the TGF- $\beta$ /DBL-1 pathway results in small body size and reduced ability to fight infection (Morita *et al.* 1999a; Suzuki *et al.* 1999; Mallo *et al.* 2002; Zugasti and Ewbank 2009). The reduced immune response was suggested to result from a failure to effectively kill and digest pathogenic bacteria (So *et al.* 2011). DBL-1 signaling regulates immune response genes and animals lacking normal DBL-1 pathway signaling have increased permeability to drugs and altered surface layers (Mallo *et al.* 2002; Roberts *et al.* 2010; Schultz *et al.* 2014). Together, this suggests loss of DBL-1 signaling impairs immune response and surface barrier protection, reducing animals' defenses against pathogen challenges. Our study aims to identify the composition of surface lipids to detect any alteration caused by genetic changes (Chapter II).

#### Advantages of the *C. elegans* model system

To study the trafficking and regulation of signaling pathways, an appropriate model organism should be complex enough to address questions that are relevant to human physiology, and simple enough to manipulate. There are several advantages to working with *C. elegans* as a model organism. The nematode has simple growth conditions and a rapid generation time. Nematode stocks can be frozen and later revived, making it easy to maintain lines of mutants. Over 3,000 mutant nematode stocks are available from the *Caenorhabditis* Genetics Center (CGC) to academic researchers. *C. elegans* hermaphrodites can either self-fertilize or mate with males. Self-fertilization

results in a clonal population of genetically identical offspring, while mating can be used to generate strains carrying multiple mutations.

In 1998, *C. elegans* was the first multicellular organism to have its genome completely sequenced. The published sequence is approximately 100 million base pairs long and contains approximately 20,000 genes. This sequence facilitated the development of a useful genetic tool available for use in *C. elegans*: RNA interference (RNAi). By feeding nematodes *E. coli* expressing double stranded RNA (dsRNA) corresponding to the sequence of the gene of interest or injecting the dsRNA directly into the worm, the function of the gene is silenced (Fire *et al.* 1998). This technique can be utilized to identify the function of individual *C. elegans* genes without the time-consuming effort of generating a mutant strain. Libraries of bacterial clones expressing dsRNA that individually target each gene in the *C. elegans* genome have been generated, allowing researchers to do reverse genetic screens for a phenotype of interest (Bargmann 2001).

These tools give us a powerful *in vivo* genetic system to study biological processes. Sydney Brenner is credited with establishing the nematode as a model system to study molecular and developmental biology through the use of genetic techniques. In his original paper, Brenner described techniques for handling *C. elegans* in the laboratory and used ethyl methane sulfonate (EMS) to induce mutations and identify an array of mutants with behavioral and growth phenotypes (Brenner 1974). Body size mutants, eventually recognized to be caused by alleles of DBL-1 pathway genes, were also identified in the original screen (Brenner 1974).

*C. elegans*, a free-living nematode that is found in temperate soil environments, feeds on bacteria. Structurally, *C. elegans* is unsegmented and bilaterally symmetrical, has a fluid-filled pseudocoelomic cavity and is protected by a tough cuticle on the exterior of the animal consisting mainly of collagen covered by lipid on the outermost surface. The digestive tract of the worm includes a mouth, pharynx, intestine and anus. Over ninety-nine percent of the *C. elegans* population is hermaphrodites, which have two ovaries, two gonad arms and a single uterus. Males make up only 0.05% of the population, and have a single-lobed gonad, vas deferens, and a specialized tail used for mating. The genome of *C. elegans* has five pairs of autosomes and one pair of sex chromosomes. Gender decision in *C. elegans* is based on an X0 sex-determination system. Hermaphrodite *C. elegans* have a matched pair of sex chromosomes (XX); males have only one sex chromosome (X0). *C. elegans* hermaphrodites can either self-fertilize or mate with males (Corsi *et al.* 2015).

After the hermaphrodite nematode lays eggs, it takes approximately 3.5 days at 20°C to complete the life cycle and reach adulthood. After hatching, *C. elegans* has four larval stages (L1- L4). In the absence of food, *C. elegans* can enter an alternative third larval stage called the dauer state; during this stage the nematodes are stress-resistant and long-lived. (Corsi *et al.* 2015). Individual nematodes have an identical pattern of cell lineage and exact number of cells for a total of 959 cells in the adult hermaphrodite and 1031 in the adult male (Sulston and Horvitz 1977). Additionally, 131 cells are eliminated by programmed cell death in the hermaphrodite during development. Once reaching

adulthood, the nematode will lay approximately 300 eggs in four days, and then has a life span of approximately 2-3 weeks.

Using *C. elegans* to test compounds for toxicity

The nematode has both mechanical and humoral innate immune defenses against infection by pathogen. Physically, a multi-layered cuticle surrounds the nematode, leaving three openings prone to infection: the mouth, anus, and vulva. *C. elegans* feeds on bacteria, and the mouth is the most common route of infection. The first barrier that the pathogen encounters is the grinder, a tri-lobed structure made of cuticle, located in the pharynx, which physically breaks down bacteria. Living bacteria that are able to pass through the grinder into the intestine are faced with a number of anti-microbial factors. The intestinal cells are known to specifically express certain lectins and proteases. The nematode also contains a number of lysozymes, which are predicted to be an important part of the immune response in the intestine (Mcghee 2007).

In our Chapter III study, we confirmed the lack of toxicity of potential nanocarrier and potential anticancer drugs in *C. elegans* by testing for organismal responses and TGF- $\beta$  signaling involvement. Due to its advantages as a research tool, *C. elegans* also makes for a practical means for studying toxic compounds. Williams and Dusenbery outlined its potential use as a screening test for neurotoxicants, including metal species, using behavioral testing (Williams and Dusenbery 1988). The use of lethality, reproduction, and behavioral tests for determining toxicity has been investigated, resulting in the determination that lethality is the least sensitive end-point, but that behavior and reproduction are much more sensitive, and yield similar results. More

recently, researchers have used *C. elegans* to elucidate the mechanisms of toxicity and the potential for various toxicants to induce alterations in expression of particular genes. Analysis of testing conditions (e.g. developmental stage, food presence, and salt content) has shown that factors such as ionic concentration of the growth medium and pH impact the results (Donkin *et al.* 1995).

As a toxicological model, *C. elegans* has been shown to be predictive of mammalian toxicity. Many studies have been conducted investigating the toxicity of various compounds including pesticides, mitochondrial inhibitors, and metals (Leung *et al.* 2008). These studies showed that the LD50 values in worms correlate with the LD50 values found in rats and mice, with results demonstrating that *C. elegans* is useful as a predictive model for neurological and developmental toxicity studies in mammalian species.

Many toxicological endpoints have been investigated using the *C. elegans* model system, including behavioral abnormalities, assessment of alterations in specific molecular pathways, genetic screening, and specific damage to the *C. elegans* nervous system. Tests that examine various behavioral endpoints and alterations in neurons and neurotransmitter systems in *C. elegans* have been developed including those that examine feeding, locomotion, memory, and movement. Using toxicants, researchers have conducted many experiments to examine behavioral outcomes following exposure. Feeding alterations decreased upon exposure to some metals and have been examined in a high-throughput manner (Boyd *et al.* 2012, Candido and Jones 1996). Chemotaxis and



altering behavior to avoid a toxicant have been observed upon exposure to some metals (Sambongi *et al.* 1999; Hilliard *et al.* 2005).

## Conclusions

Overall, our studies give a better idea of regulation of TGF- $\beta$ /DBL-1 trafficking in the secreting cell, implicating intracellular vesicle-associated molecules caveolin CAV-1 and small GTPase UNC-108/RAB-2, but not autophagy-associated protein BEC-1, in DBL-1 trafficking (Chapter II). We also studied the changes in surface barrier associated with TGF- $\beta$ /DBL-1 pathway (Chapter II). We analyzed and established lack of toxicity in *C. elegans* to three potential nanocarrier compounds and two potential anti-cancer compounds, thus validating their testing in higher organisms (Chapter III).

Using the *C. elegans* system, we also showed insulin signaling is not required for the environmental sensing phenotypes associated with loss of tectorin-like ZP-domain protein DYF-7 (see Appendix I). This work provides insight into progressive deafness caused by tectorin defects, suggesting a mechanical cell anchoring defect is sufficient to cause neuronal defects without the need for downstream signaling pathway involvement.

## CHAPTER II

### DBL-1 TRAFFICKING AND ITS ROLE IN CHANGING THE SURFACE BARRIER OF *C. ELEGANS*

#### Introduction

Transforming growth factor beta (TGF- $\beta$ ) is a superfamily of proteins involved in signaling that regulates a variety of cellular processes, including stress responses, proliferation, and determination of developmental fate, during embryogenesis as well as in mature tissues, in organisms from nematodes and flies to mammals (Wu and Hill 2009). There have been instances where the TGF- $\beta$  pathway has been linked to environmental stress responses (Kang *et al.* 2003; Yoshimura *et al.* 2010; Walshe *et al.* 2013; Huang *et al.* 2015; Wu *et al.* 2015).

Owing to the complexity of human systems, we use the nematode model organism *Caenorhabditis elegans* (*C. elegans*), which has a small size and short reproductive cycle, is free living and easy to maintain, and has an almost transparent body type that make it a practical model for study (Brenner 1974). Also, many molecular disease and stress response pathways are conserved in this organism. Developing *C. elegans* as a model attenuates the need to use vertebrate animals in preliminary stress-response testing (Candido and Jones 1996; Boyd *et al.* 2012). *C. elegans* has only five TGF- $\beta$  ligands with non-redundant, non-lethal functions, which share at least 70% homology with human TGF- $\beta$  pathway members (Lai *et al.* 2000; Patterson and Padgett

2000; Gumienny and Savage-Dunn 2013). TGF- $\beta$  signaling pathways are highly conserved at both the molecular and functional level, and the homologs of regulators identified in *C. elegans* have been shown to be used by more complex organisms in a related fashion (see Table 2.1). These factors make *C. elegans* a suitable model organism to study this pathway (Gumienny and Savage-Dunn 2013).

The *C. elegans* TGF- $\beta$ /DBL-1 pathway is involved in maintaining body size and, in part, cuticle composition, which helps protect animals from environmental stresses (see Figure 2.1). The exact cells in which DBL-1, TGF- $\beta$  ligand in *C. elegans*, is expressed and the entire regulation of DBL-1 trafficking remains unverified. DBL-1 was

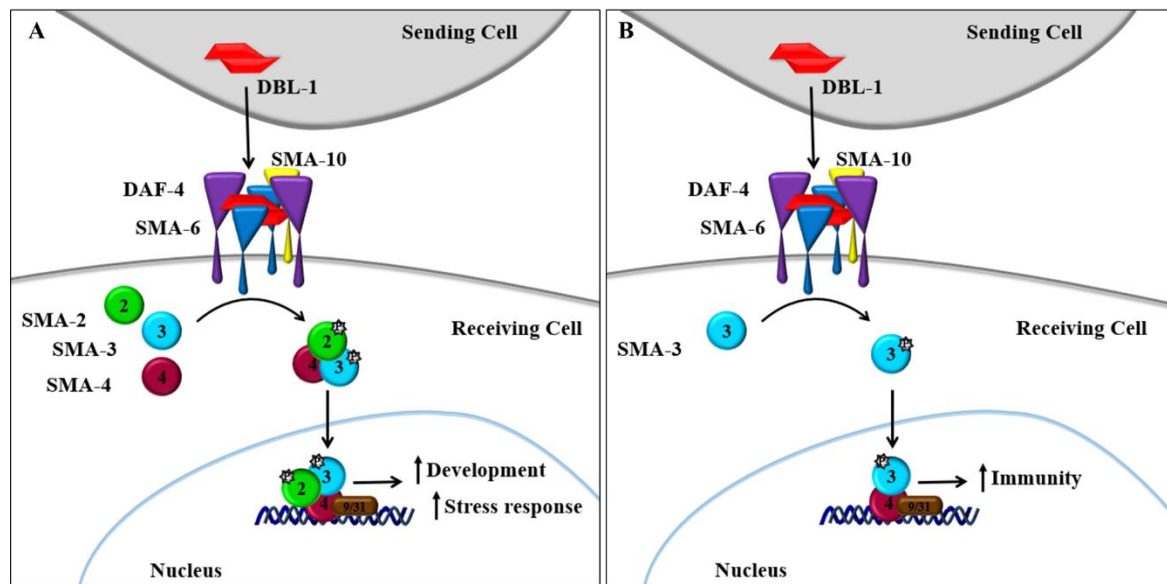


Figure 2.1. Canonical and non-canonical TGF- $\beta$ /DBL-1 signaling pathway in *C. elegans*. The DBL-1 signal (red) is received by a heterotetrameric receptor composed of two SMA-6 type I receptor and two DAF-4 type II receptor subunits (blue and purple, respectively). The DBL-1 signal is transduced by SMA-2, SMA-3, and SMA-4 Smads. Transcription factors (browns) that act with Smads to carry out DBL-1-mediated responses include SMA-9/Schnurri, LIN-31/forkhead, and MAB-31. A. Canonical TGF- $\beta$ /DBL-1 pathway promotes development and stress response through SMA-2, SMA-3, and SMA-4. B. Non-canonical TGF- $\beta$ /DBL-1 pathway promotes immune responses only by SMA-3, independent of SMA-2 and SMA-4. Image adapted from Gumienny and Savage-Dunn (2013).

previously reported to be expressed in the AFD amphid neuron, the ventral cord neurons VA, VB, DA, and DB neurons in the pharyngeal region, canal associated neuron (CAN), and body wall muscles (Morita *et al.* 1999). Our study will help us better elucidate the expression localization of DBL-1.

Component	<i>C. elegans</i> gene name	<i>Drosophila</i> gene name	Human gene name	Molecule or family
Ligand	<i>dbl-1</i>	<i>dpp</i>	BMP5	Transforming Growth Factor- $\beta$
	<i>daf-7</i>	<i>dawdle</i>	GDF11	
	<i>unc-129</i>	-	-	
	<i>tig-2</i>	<i>gbb</i>	BMP8	
	<i>tig-3</i>	dActivin	BMP2	
Type I receptor	<i>sma-6</i>	<i>tkv</i>	BMPRIB	
	<i>daf-1</i>	<i>babo</i>	TGF-bRI	
Type II receptor	<i>daf-4</i>	<i>put</i>	ACTRIIB	ser/thr kinase receptor

Table 2.1. TGF- $\beta$  superfamily signaling is conserved in eukaryotes. Adapted from (Gumienny and Savage-Dunn 2013)

To identify potential regulators of DBL-1 trafficking, we used a functional GFP-tagged DBL-1 RNAi screen and selected candidates based on previous studies. (Mallo *et al.* 2002; Zugasti and Ewbank 2009; Roberts *et al.* 2010; Beifuss and Gumienny 2012).

We chose three genes, *unc-108/rab-2*, *cav-1*, and *bec-1*, and, because RNAi-depletion of each of these intracellular vesicle transport genes severely affected the fluorescence intensity of GFP-tagged DBL-1 (see Table 2.2). Caveolin has been reported to be important for membrane invagination during vesicle trafficking and it associates with lipid rafts to form caveolae that are largely involved in signal transduction to the plasma membrane (Patel 2009). RAB2A has been reported to play a crucial role in vesicular

transport from the endoplasmic reticulum to the Golgi complex (Tisdale *et al.* 1992). It has also been identified as a regulator of postendocytic trafficking in both neurons and coelomocytes at the level of early or recycling endosomes (Chun *et al.* 2008). In *C. elegans*, *unc-108/rab-2* acts in neurons and engulfing cells to control locomotion and cell corpse removal, respectively, indicating that *unc-108* has distinct roles in different cell types (Mangahas 2008). BEC-1 is orthologous to mammalian autophagy proteins Atg6/Vps30/Beclin1. It plays a key role in retrograde transport of endocytic vesicles to the Golgi, phagosome maturation, cell corpse clearance, and retrograde transport of MIG-14/Wntless to the lysosome (Ruck *et al.* 2011).

Candidate gene	Homolog in humans	Known functions
<i>unc-108/rab-2</i>	<i>rab2a</i> (GTPase)	Vesicle fusion and trafficking
<i>cav-1</i>	<i>cav1</i> (caveolin)	Endocytosis, protein scaffolding
<i>bec-1</i>	<i>bec1</i> (beclin)	Vesicle trafficking, regulation of autophagy and cell death

Table 2.2. Genes studied, their homologs, and their major known functions

Animals lacking DBL-1 (*dbl-1(-)*) and animals overexpressing DBL-1 (*dbl-1(++)*) have decreased and increased body lengths respectively (Schultz *et al.* 2014). Schultz *et al.* showed using transmission electron microscopy that there are differences in the lipid layer of the epicuticle of the animals, which seems to play an important role in the worm-star phenotype and may explain the increased sensitivity of animals lacking DBL-1 to immune challenges (see Figure 2.2A-C) (Schultz *et al.* 2014). Previous work in the Gumienny laboratory also showed that animals lacking TGF- $\beta$ /DBL-1 signaling

can form worm-stars, a phenomenon where hermaphrodites' whip-like tails can become entwined in liquid (see Figure 2.2D) (Schultz *et al.* 2014).

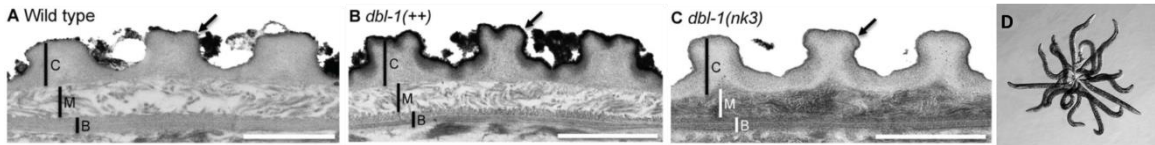


Figure 2.2. TEM micrographs of differences in amount of lipids in *C. elegans* strains A. Wild-type, B. *dbl-1(++)*, and C. *dbl-1(-)*. D. Representative image of a worm-star. Adapted from Schultz *et al.* (2014).

These different phenotypes arise from either the canonical TGF- $\beta$ /DBL-1 signaling pathway or the non-canonical signaling pathway (see Figure 2.1). The canonical pathway includes Smads SMA-2, SMA-3 and SMA-4 whereas the non-canonical pathway is independent of SMA-2 and SMA-4. The non-canonical pathway was determined to be involved in fungal infection response (Hodgkin *et al.* 2013). There has been no significant study relating the TGF- $\beta$ /DBL-1 pathway to other stress responses as of yet, however, studies in other models give support that it is a field to be explored.

## Materials and Methods

### Strains and maintenance

*C. elegans* strains that were used in these studies are derived from the wild-type variety Bristol strain N2 and cultured on nematode growth media (NGM) plates as previously described (Brenner 1974). All strains were cultured on *E. coli* strain OP50 at 20°C, except where noted. Strains used include: N2 (wild type), TLG182 *tex1s100 [dbl-1p::dbl-1:gfp + ttx-3p::rfp]* IV (also referred to as *dbl-1(++)*), NU3 *dbl-1(nk3)* V (also referred to as *dbl-1(-)*), CB502 *sma-2(e502)* III, TLG634 *sma-3(wk30)* III, DR1369 *sma-*

4(e729) III, VC2197 *sma-6(ok2894)* II, TLG368 *vsIs48 (unc-17p::gfp); texEx182 (dbl-1p::dsRed2-E5 + ttx-3p::rfp)*, TLG627 *dbl-1(nk3) [dbl-1p::dbl-1:mrfp; dbl-1p::cav-1:gfp + ttx-3p::rfp]* , TLG638 *dbl-1(nk3) [dbl-1p::dbl-1:mrfp; bec-1p::bec-1:gfp + ttx-3p::rfp]*, and TLG675 *texEx448 [dbl-1p::dbl-1:mrfp; unc-108p::unc-108:gfp + ttx-3p::gfp]*.

#### Microscopy analysis

Animals were grown to the required developmental stage, anesthetized using 1 mM levamisole hydrochloride (Sigma, St. Louis, MO), and imaged using a Nikon A1R-A1 confocal system with a Nikon Eclipse Ti inverted microscope and Nikon NIS elements AR-3.2 imaging software (Nikon Instruments, Melville, NY). Microscopic observations were standardized to bring the fluorescence intensity values in measurable dynamic range. Animals were imaged at 60X magnification for fluorescence intensity. Image capturing conditions were kept constant for each experiment.

#### *dbl-1* expression analysis

To determine which neurons express *dbl-1*, we used a strain (TLG368) that expresses green fluorescent protein from the *unc-17* promoter in all cholinergic neurons and a red fluorescent protein (*dsRED2-E5*) from the *dbl-1* promoter. We observed the cells in the VNC in which we could see green and red fluorescence to determine if the DBL-1 expressing cells were cholinergic by imaging using the Nikon A1 confocal microscope and Nikon NIS Elements software. All stages of animals were observed, with a total of  $n > 30$ .

## Colocalization Studies

Sequence encoding fluorescent proteins were fused to candidate genes of interest by standard molecular cloning techniques and expressed in strains expressing GFP-tagged DBI-1 were used. At least five larval stage four (L4) animals were observed for each experiment. Animals were imaged and statistically analyzed as described above. Statistical analysis was done using the Pearson correlation function of the Nikon NIS Elements AR-3.2 imaging software. Pearson correlation was used to analyze the linear correlation between the two proteins. Pearson's correlation coefficient (PCC) values range from 0 to 1 and are categorized as follows: 0 - 0.19 "very weak", 0.20 - 0.39 "weak", 0.40 - 0.59 "moderate", 0.60 - 0.79 "strong", 0.80 - 1.0 "very strong".

## Worm-star formation assays

Worm-star formation assays were conducted as previously described (Schultz *et al.* 2014). Staged adult animals were washed in M9 buffer two or three times to remove residual bacteria. Animals were then incubated for three to twenty hours at room temperature or 25°C in 3 to 7.5 ml M9 buffer (without OP50 bacteria) in 60 mm petri dishes tilted at a slight angle to concentrate animals in a single area of the plate. The number of animals in worm-star aggregations, clusters of two or more animals entangled at their tails, was quantified for each genotype by visual inspection using a dissecting microscope. Three independent trials were performed, and results were pooled, with approximately 300 to 30,000 animals per trial for each genotype. Worm-stars were imaged at 60X magnification using iVision-Mac software (BioVision Technologies,



Exton, PA) and a Retiga-2000R CCD camera mounted on a Nikon SMZ1500 dissecting microscope.

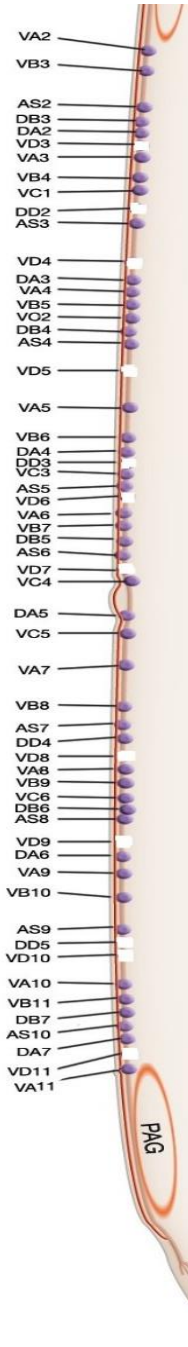
#### Surface barrier analysis

Surface lipids were extracted from the worms using a mild chloroform-methanol extraction method (Daugherty and Lento 1983), transmethylated, and analyzed by gas chromatography-flame ionization detection (GC-FID) using a Hewlett Packard HP 5890 II plus GC instrument and ChemStation software. Assays were performed with wild-type, *dbl-1(-)*, and *dbl-1(++)* strains.

#### Results

##### DBL-1 localizes to cholinergic ventral cord neurons of *C. elegans*

Using different promoter regions, Morita et al., showed that the DBL-1 ligand was expressed in a subset of cholinergic ventral cord neurons, but also other cells (Morita et al. 1999b). To confirm the cells that express DBL-1, we generated the strain TLG368, which has all cholinergic neurons marked with green fluorescent protein (GFP) and cells that express DBL-1 marked red with a red fluorescent protein under the control of the 1.38 kb promoter sequence upstream of *dbl-1*. This red protein, dsRED-E5, in other systems starts green but changes to red over time. However, we did not observe the nascent green dsRED-E5 species from the transgene expressing it before we crossed it into the background expressing *unc-17p::gfp*. We looked at L1 to adult stages of *C. elegans* and confirmed that our promoter expresses in all the cholinergic ventral cord neurons. We also confirmed lack of *dbl-1* expression in any of the GABAergic neurons (Schultz and Gumienny, unpublished). The lateral neuron CAN also expresses *dbl-1*.



VNC neuron	Overall DBL-1 expression (Y/N)	Adult		L4		L3 n=5 (%)	L2 n=7 (%)	Dauer n=3 (%)	L1 n=1 (%)
		Hermaphrodite n=6 (%)	Male n=4 (%)	Hermaphrodite n=5 (%)	Male n=2 (%)				
AS1	Y	33	25	20	100	20	43	100	N.A
AS2	Y	50	75	40	0	40	57	33	N.A
AS3	Y	33	75	60	100	20	43	33	N.A
AS4	Y	67	50	20	100	40	43	33	N.A
AS5	Y	50	50	40	100	60	43	67	N.A
AS6	Y	33	75	60	0	20	14	67	N.A
AS7	Y	50	25	60	100	60	43	100	N.A
AS8	Y	50	50	100	100	60	14	67	N.A
AS9	Y	50	50	60	100	40	86	100	N.A
AS10	Y	67	50	80	100	20	57	67	N.A
AS11	Y	0	25	40	50	20	29	33	N.A
DA1	Y	50	25	20	50	40	29	33	100
DA2	Y	50	100	40	100	40	57	67	100
DA3	Y	50	75	20	50	60	29	67	100
DA4	Y	50	75	60	0	60	57	100	100
DA5	Y	83	100	80	100	60	71	67	100
DA6	Y	83	50	60	0	40	14	67	100
DA7	Y	67	50	80	100	20	29	100	100
DA8	Y	33	25	60	50	40	57	33	100
DA9	Y	17	25	20	50	20	14	67	100
DB1	Y	33	25	20	50	40	29	33	100
DB2	Y	50	50	60	50	20	29	67	100
DB3	Y	50	100	20	0	40	57	33	100
DB4	Y	67	50	20	50	40	29	33	100
DB5	Y	50	75	60	100	20	29	100	100
DB6	Y	50	50	40	50	20	14	67	0
DB7	Y	67	50	60	50	20	29	67	100
VA1	Y	50	25	40	50	20	29	100	100
VA2	Y	33	50	60	0	40	57	33	0
VA3	Y	50	50	60	50	60	29	67	0
VA4	Y	50	75	20	0	40	29	33	0
VA5	Y	33	25	60	100	40	57	67	0
VA6	Y	33	50	80	50	20	14	100	0
VA7	Y	83	50	80	0	60	29	33	0
VA8	Y	50	50	60	50	20	0	33	0
VA9	Y	67	50	80	100	40	71	100	0
VA10	Y	50	50	40	50	20	43	100	0
VA11	Y	33	50	40	50	20	57	100	0
VA12	Y	0	25	20	0	0	29	0	0
VB1	Y	17	25	40	100	60	43	67	N.A
VB2	Y	33	0	20	100	40	43	33	N.A
VB3	Y	33	50	60	0	60	86	33	N.A
VB4	Y	33	75	80	100	40	29	67	N.A
VB5	Y	50	75	20	0	40	14	33	N.A
VB6	Y	50	25	60	50	40	43	33	N.A
VB7	Y	67	50	80	0	20	14	100	N.A
VB8	Y	50	25	80	50	40	14	67	N.A
VB9	Y	50	50	60	50	20	14	67	N.A
VB10	Y	67	25	40	50	20	57	67	N.A
VB11	Y	67	50	60	50	20	43	100	N.A
VC1	Y	33	75	80	50	40	29	67	N.A
VC2	Y	67	75	20	100	40	29	33	N.A
VC3	Y	50	50	60	100	40	57	67	N.A
VC4	Y	67	75	60	50	80	57	33	N.A
VC5	Y	83	100	100	100	60	43	67	N.A
VC6	Y	33	50	60	50	20	14	67	N.A

Table 2.3. Expression of DBL-1 in ventral nerve cord (VNC) cells with reference figure of the VNC cells. Purple cells represent cholinergic motor neurons in which *unc-17* is expressed. No co-localization with GABAergic neurons was observed (not shown). The figure is adapted from WormAtlas Altun and Hall (2011).

We observed and verified DBL-1 expression in VA, VB, DA, DB, and CAN cells as Morita *et al.* showed. Expression of DBL-1 and UNC-17 in a particular cell in more than one stage of the animal confirms localization in that cell. However, we also observed expression in ventral nerve cord cells, VC and AS. This expression pattern appears to be consistent from L1 to adult hermaphrodites, as well as in males and in dauers (see Table 2.3). *dbl-1p::dsRed:dbl-1* was expressed only in the VNC cells that also expressed *unc-17p::GFP*, not in DD and VD GABAergic neurons that also comprise the VNC. Previous work in our lab using a GABAergic neuronal marker confirmed that there was no DBL-1 expression in DD or VD cell bodies and did not detect any expression in the AFD, the pharyngeal region, or body wall muscles. Thus, we verified DBL-1 expression in cholinergic motor neurons.

#### UNC-108/Rab GTPase and DBL-1/TGF- $\beta$ colocalize

UNC-108, a small GTPase known as RAB2A in plants and mammals, has also been identified as a regulator of postendocytic trafficking and apoptosis (Chun *et al.* 2008; Mangahas 2008). It has been also been reported to play a crucial role in vesicular transport from the endoplasmic reticulum to the Golgi complex (Tisdale *et al.* 1992; Cheung *et al.* 2002; Sumakovic *et al.* 2009). Previous work from our lab involving RNA inhibition of *unc-108* showed that the localization of DBL-1 was affected; punctate DBL-1 was reduced in the nerve cord. We investigated the role of UNC-108 as a potential regulator of DBL-1 trafficking by observing for colocalization of mRFP-tagged DBL-1 and GFP-tagged UNC-108.

The strength of colocalization was determined with the Pearson's correlation coefficient to be  $0.78 \pm 0.04$  SD indicating a strong level of colocalization between DBL-1 and UNC-108 (see Figure 2.3). Hence, this work provides evidence that UNC-108 is directly associated with DBL-1 vesicles.

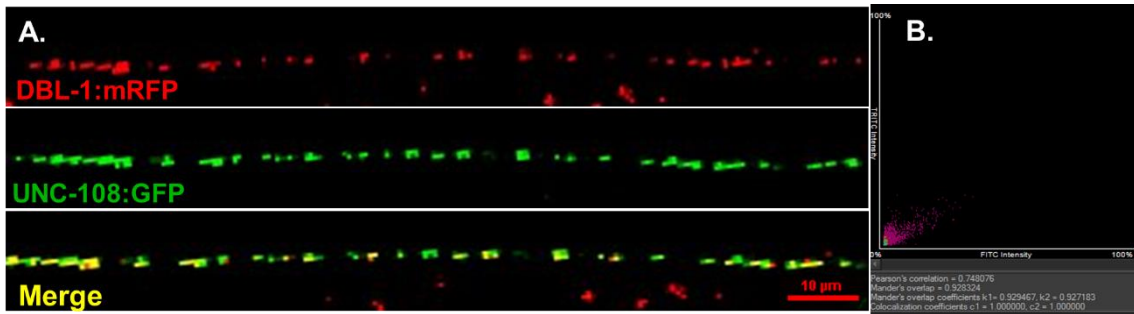


Figure 2.3. Colocalization of UNC-108 and DBL-1. A. Shows panels of UNC-108:GFP (green), DBL-1:mRFP (red), and the merged image (yellow). B. Shows a scatterplot of red fluorescence (Y-axis) vs green fluorescence (X-axis) used to calculate the Pearson's correlation  $r$ -value = 0.75, indicating a strong ( $0.6 < r < 0.79$ ) correlation.

#### CAV-1/caveolin and DBL-1/TGF- $\beta$ colocalize

Major roles for caveolin have been identified in forming vesicles from Golgi membrane and also from plasma membrane for endocytosis (Patel 2009). Previous work from our lab involving RNA inhibition of *cav-1* showed that the localization of DBL-1 was affected; punctate DBL-1 was not seen in the nerve cord. Caveolin is associated with cholesterol-enriched lipid rafts in membranes and dietary cholesterol depletion makes GFP- tagged DBL-1 cords fainter, phenocopying *cav-1* RNAi, and supporting the model that this function of caveolin requires cholesterol. Furthermore, *cav-1(-)* animals were  $88 \pm 2\%$  wild-type body length, similar to loss of DBL-1. CAV-1 was found to colocalize with DBL-1 homolog BMP-4.

We investigated the role of caveolin as a potential regulator of DBL-1 trafficking by observing for colocalization of mRFP-tagged DBL-1 and GFP-tagged CAV-1 in live animals. We observed that punctate DBL-1 exhibited nearly complete colocalization with CAV-1. The strength of colocalization was determined with the Pearson's correlation coefficient as calculated by NIS Elements to be  $0.82 \pm 0.05$  SD, indicating a very strong level of colocalization (see Figure 2.4). These results suggest that DBL-1 is in CAV-1-positive vesicles.

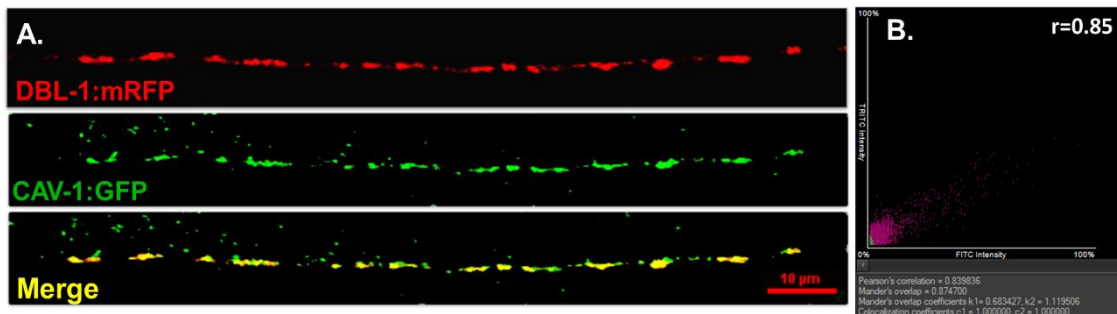


Figure 2.4. Colocalization of CAV-1 and DBL-1. A. Shows panels of CAV-1:GFP (green), DBL-1:mRFP (red), and the merged image (yellow). B. Shows a scatterplot of red fluorescence (Y-axis) vs green fluorescence (X-axis) used to calculate the Pearson's correlation  $r$ -value= 0.84, indicating a very strong ( $r > 0.8$ ) correlation.

BEC-1/beclin1 autophagy-related protein and DBL-1/TGF- $\beta$  do not colocalize

BEC-1 has known roles in retrograde transport of endocytic vesicles to the Golgi, phagosome maturation, cell corpse clearance, and retrograde transport of MIG-14/Wntless to the lysosome (Ruck *et al.* 2011). *bec-1* mutants are small, comparable to *dbl-1* pathway mutants (Aladzcity *et al.* 2007). Previous work from our lab involving RNA inhibition of *bec-1* showed that the localization of DBL-1 was affected; punctate DBL-1 was reduced in the nerve cord. We investigated the role of BEC-1 as a potential regulator of DBL-1 trafficking by observing for colocalization of mRFP tagged DBL-1

and GFP-tagged BEC-1. We observed that BEC-1 exhibited negligible colocalization with punctate DBL-1. The strength of colocalization was determined with the Pearson's correlation coefficient to be  $0.2 \pm 0.06$  SD, indicating a weak level of colocalization (see Figure 2.5). These results suggest that BEC-1 does not directly play a role in regulation of DBL-1 vesicle trafficking.

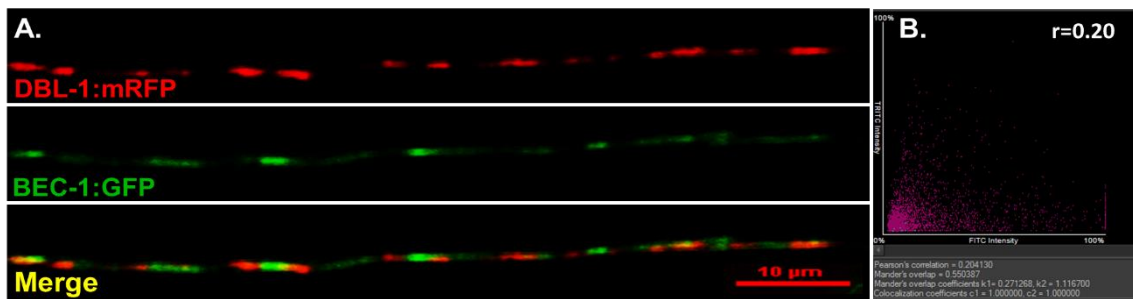


Figure 2.5. Colocalization of BEC-1 and DBL-1. A. Shows panels of BEC-1:GFP (green), DBL-1:mRFP (red), and the merged image (yellow). B. Shows a scatterplot of red fluorescence (Y-axis) vs green fluorescence (X-axis) used to calculate the Pearson's correlation  $r$ -value = 0.2, indicating a weak ( $0.2 < r < 0.39$ ) correlation.

*dbl-1*/TGF- $\beta$  strains form worm-stars and lipid composition of their surface barrier is different from wild-type

In liquid media, *dbl-1*(-) worms sometimes stick together by their tail and form star-like structures called worm-stars. TEM images of cuticle surface showed differences in lipid composition between wild-type and *dbl-1*(-) strains (Schultz *et al.* 2014). To confirm our hypothesis that DBL-1 signaling plays a role in worm-star formation by causing differences in surface barrier composition of *C. elegans*, we first tested for worm-star formation in wild-type and *dbl-1* pathway mutant strains. We observed that wild-type and *dbl-1*(++) strains never formed worm-stars. Whereas, we observed worm-star formation in *dbl-1*(-) and other downstream pathway mutants, *sma-2*, *sma-3*, *sma-4*,

and *sma-6* at least four out of 6 times (see Table 2.4). This result indicates that the canonical DBL-1 signaling pathway plays a role in worm-star formation.

We then tested for variation in lipid surface barrier composition between wild-type and *dbl-1(-)* *C. elegans*. First, we optimized a protocol that mostly isolates surface lipids from internal lipids. Then we showed that a protocol for transesterification of the lipid species is effective to allow them to be detected by gas chromatogram – mass spectroscopy (GC-MS). We developed the protocol by employing a mild chloroform-methanol treatment to the worms, conducting thin layer chromatography, and finally detecting the surface lipids via GC-MS. At least three trials were performed to get notable preliminary results.

Preliminary chromatogram results showed a difference in short chain fatty acids between the surface barriers of the two strains tested (see Figure 2.6). This suggests that DBL-1 signaling affects the lipid surface barrier composition in *C. elegans*.

Strain	Worm-star formation (+/-)					
	Trial 1	Trial 2	Trial 3	Trial 4	Trial 5	Trial 6
<b>WT</b>	-	-	-	-	-	-
<b><i>dbl-1(++)</i></b>	-	-	-	-	-	-
<b><i>dbl-1(-)</i></b>	+	+	+	+	+	+
<b><i>sma-2</i></b>	-	+	+	+	-	+
<b><i>sma-4</i></b>	+	+	+	+	+	+
<b><i>sma-6</i></b>	-	+	+	+	+	+

Table 2.4. Worm-star formation occurs in DBL-1 pathway mutants. Assays were performed with WT, *dbl-1(-)*, *dbl-1(++)*, *sma-2*, *sma-3*, *sma-4*, and *sma-6* strains. Values are qualitative conclusions from at least 6 independent experiments ( $n > 300$  animals) for each condition.

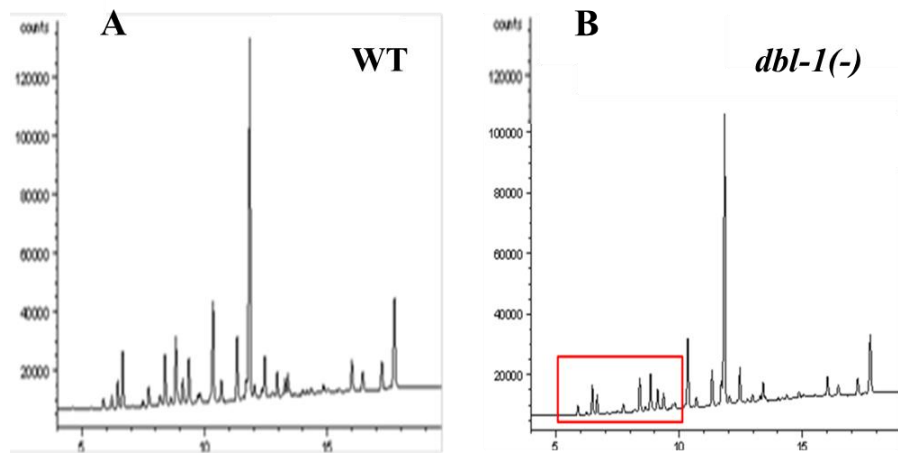


Figure 2.6. Representative GC-FID chromatograms of surface lipids of A. wild-type (N2) and B. *dbl-1(nk3)* surface barriers. The red box highlights differences in acyl moieties between the two strains.

## Discussion

We looked at and confirmed that our promoter expresses in all the cholinergic ventral cord neurons and none of the GABergic neurons from L1 through adult stages of *C. elegans*. The *C. elegans* embryo hatches at 800 minutes and the general body plan does not change post-embryonically. The larvae remain in the L1 stage for approximately 12 hours (720 mins). At L1 stage, only DA, DB and VA1 ventral cord neurons will be seen. DBL-1 in *C. elegans* was previously reported to be expressed in the AFD amphid neuron, the cell bodies of the ventral cord neurons such as VA, VB, DA and DB, neurons in the pharyngeal region, canal associated neuron (CAN), and body wall muscles (Morita *et al.* 1999b). Morita *et al.* also observed male-specific expression in the tail region. They stated that the expression pattern persists from the L1 to adult hermaphrodite stage. The difference in expression might arise from the additional (~) 4 kb upstream sequence to the *dbl-1* promoter included in their gene expression, whereas we have 1.38 kb of upstream sequence. In conclusion, we have verified the exact cells that express DBL-1 in



the VNC. Because the neuronal wiring diagram of *C. elegans* is known, this expanded DBL-1 expression pattern may help us understand how cells that secrete DBL-1 receive regulatory cues from environmental sensing or other neurons.

Rab proteins are known regulators of specific aspects of vesicular transport at specific sites in eukaryotes and RAB2A (UNC-108 in *C. elegans*) has been reported to be play a crucial role in vesicular transport from the endoplasmic reticulum to the Golgi complex, postendocytic trafficking, locomotion, and cell corpse removal (Tisdale *et al.* 1992; Chun *et al.* 2008; Mangahas 2008; Gallegos *et al.* 2012). Lack of UNC-108 causing reduced fluorescence of DBL-1 in vesicles provides evidence that UNC-108 is involved in transport of DBL-1 to the plasma membrane. The colocalization of UNC-108 with DBL-1 supports the hypothesis that DBL-1 is transported from the endoplasmic reticulum to the Golgi complex via vesicular transport assisted by UNC-108.

Caveolins have previously been reported to be involved in microtubule transport and kiss-and-run kinetics of caveolin associated vesicles (Pelkmans 2005; Parkar *et al.* 2009). The reduced body length of *cav-1(-)* animals as compared to wild-type suggests that caveolin affects DBL-1 signaling. Reduction in fluorescence of DBL-1 caused by lack of caveolin provides further evidence that caveolin is involved in transport of DBL-1 to or from the plasma membrane. The lack of cholesterol causing disruption in expression of DBL-1, phenocopying *cav-1* RNAi, suggests that cholesterol is essential for proper functioning of caveolin (Beifuss and Gumienny, unpublished). The work presented here shows a high level of colocalization of CAV-1 and DBL-1 in living animals. We conclude that DBL-1 is transported in caveolin-coated vesicles from the Golgi complex

to the plasma membrane along microtubules and also in the kiss-and-run dynamics at the plasma membrane for release of DBL-1.

BEC-1 has known roles in retrograde transport of endocytic vesicles to the Golgi, phagosome maturation, cell corpse clearance, and retrograde transport of MIG-14/Wntless to the lysosome (Ruck *et al.* 2011). *bec-1* mutants are small, similar to *dbl-1* pathway mutants (Aladzsity *et al.* 2007). Because loss of BEC-1 reduced fluorescence levels of GFP-tagged DBL-1, we tested if DBL-1 was recycled with the help of BEC-1. However, minimal colocalization of UNC-108 with DBL-1 led us to conclude that BEC-1 does not play a direct role in regulating DBL-1 trafficking.

We confirmed that worm-star formation is a DBL-1 associated phenotype. Because the non-canonical DBL-1 pathway is used to mount an innate immune response to the fungus *D. coniospora*, we asked if canonical or non-canonical DBL-1 signaling is required for a possibly related *dbl-1* phenotype, worm-star formation. (Hodgkin *et al.* 2013). Our results give evidence of the canonical DBL-1 signaling pathway playing a role in worm-star formation. Preliminary lipid surface composition chromatograms which show differences in lipid profiles, suggest that DBL-1 signaling may be required for proper lipid composition of the surface barrier. This work has also established the basis of determining the composition of lipid surface barrier in *C. elegans* by developing a novel protocol to extract only surface lipids. Ms. Madhu and Dr. Faure, members of TWU Biology research community, have further optimized the protocol to efficiently extract and analyze surface lipids. Further testing and comparing lipid profiles of wild-

type with other DBL-1 pathway mutants will confirm our hypothesis and also help us explore specific lipids on the surface barrier as anthelmintic drug target.

## CHAPTER III

### ROLE OF *C. ELEGANS* DBL-1 IN GENERATING AN ORGANISMAL STRESS RESPONSE TO TEST COMPOUNDS

#### Introduction

Changes from routine that cause an imbalance of any sort can be perceived by animals as stress, and they cope by responding to it with a variety of “stress responses”. Unsurprisingly, stress can lead to death; the American Psychological Association showed that stress is linked to the six leading causes of death: heart disease, cancer, lung ailments, accidents, cirrhosis of the liver, and suicide. Also, about 75% of all physician office visits are for stress-related ailments (Simmons S. P. 1997; Tennant 1999; Salleh 2008). Studies show that animals respond to environmental stressors at organismal, cellular, and molecular levels (Kassahn *et al.* 2009; Fulda *et al.* 2010; Kagias *et al.* 2012).

Transforming growth factor beta (TGF- $\beta$ ), a *Caenorhabditis elegans* DBL-1 homolog, is a superfamily of signaling proteins that regulates a variety of cellular processes, including stress responses, proliferation, and determination of developmental fate, during embryogenesis as well as in mature tissues. The signaling pathway is conserved in organisms such as nematodes and flies to mammals (Wu and Hill 2009). The TGF- $\beta$  pathway has been linked to environmental stress directly or indirectly by pathway cross-talk (Guo and Wang 2009). The TGF- $\beta$  pathway boosts stress response in human epithelial cells by repressing inhibitors of differentiation (Kang *et al.* 2003).

Upregulation of TGF- $\beta$  pathway members was observed when mice were exposed to titanium nanoparticles that caused renal fibrosis by oxidative stress (Huang *et al.* 2015). Kidney fibrosis and oxidative stress responses were suppressed by TGF- $\beta$  pathway signaling *in vivo* and *in vitro* (Wu *et al.* 2015). Shear stress on umbilical cells induced TGF- $\beta$  signaling (Walshe *et al.* 2013). TGF- $\beta$  signaling plays a role in balancing immunity and tolerance by inducing production of T-cells and interleukins as well as suppressing inflammatory stress responses (Yoshimura *et al.* 2010).

Owing to the complexity of human systems as well as various ethical issues, it can be difficult to test the anatomical and physiological effect of a stressor. However, *C. elegans* is an established organismal biosensor for environmental stress screening. This roundworm has a small size and short reproductive cycle, is free living and easy to maintain, and has an almost transparent body type that make it a practical model for study. Also, many molecular disease and stress response pathways are conserved in this organism which attenuates the need to use vertebrate animals in preliminary stress-response testing. *C. elegans* responds to a diverse set of challenges, including high salt concentration, changes in osmolarity, bacterial and fungal infection, hypoxia, changes in pressure, quantum-dots (q-dots), and drugs (Candido and Jones 1996; Schouest *et al.* 2009; Boyd *et al.* 2012; Rodriguez *et al.* 2013). *C. elegans* has also been used to determine the toxicity effects of various compounds, including nanocarriers, anti-cancer drugs, and metallopolymers (Kaletta and Hengartner 2006; Bae *et al.* 2012; Charoenphol and Bermudez 2014; Kobet *et al.* 2014; Kyriakakis *et al.* 2015). This body of work

validates *C. elegans* as an accepted model for toxicity testing and for identifying molecular stress response pathways.

*C. elegans* has only five TGF- $\beta$  ligands with non-redundant, non-lethal functions that share at least 70% homology with human TGF- $\beta$  pathway members (Lai *et al.* 2000; Patterson and Padgett 2000; Gumienny and Savage-Dunn 2013). TGF- $\beta$  signaling pathways are highly conserved at both the molecular and functional level, and the homologs of regulators identified in *C. elegans* have been shown to be used by more complex organisms in a related fashion (Gumienny and Savage-Dunn 2013). The TGF- $\beta$ /DBL-1 pathway is involved, in part, in maintaining body size and cuticle composition, which helps protect animals from environmental stresses. Animals lacking DBL-1 (*dbl-1(-)*) and animals overexpressing DBL-1 (*dbl-1(++)*) have decreased and increased body lengths respectively (Schultz *et al.* 2014). Therefore, body size can be used to determine the involvement of DBL-1 signaling. These factors demonstrate the suitability of using *C. elegans* as a model organism to study the role of this pathway in responding to stresses.

It has been shown that inactivation of mammalian TGF- $\beta$  receptor II contributes to malignant transformation at an early step of tumorigenesis and it is regulated by histone acetyltransferases (HATs), enzymes that assist in decompaction of chromatin (Park *et al.* 2002). Amidoximes are chemical compounds that have been determined to be anti-cancerous in model systems such as mice and rats by inhibiting HATs and HDACs (histone deacetylases) (Flora *et al.* 1978). The Bergel lab has shown that novel amidoxime compounds have low toxicity with high efficacy *in vitro* (Bergel, in preparation). I tested two of Bergel lab amidoximes in the *in vivo* model *C. elegans*. This

work will provide valuable direction on the usefulness of the compound as a potential anti-cancer drug. It will help us in elucidating the effect of the compound, if any, on DBL-1 signaling and identify the exact molecular target of the drug to help us understand the pathway better.

Nanocarriers can be described as delivery systems that carry another substance, such as a drug. They can be of different types and materials, such as micelles, polymers, liposomes, and carbon-based materials. Nanocarriers, which are small in size, and contain drugs that can be delivered to a specific target, seem to be one of the ideal solutions as they provide enhanced permeability and retention (Ghosh *et al.* 2009; Ghoshmitra *et al.* 2011a; Ghoshmitra *et al.* 2011b; Ghoshmitra *et al.* 2012; Ghoshmitra *et al.* 2013). Like drugs, nanocarriers need to be tested for biocompatibility to avoid adverse organismal responses. In collaboration with the Hynds lab, I tested fluorescent potential nanocarriers, based on q-dots, on *C. elegans*. It will help us determine if the potential nanocarrier shell itself generates any harmful effects in the animal so that it gives our collaborators a basis for the decision of testing them in mammals. It may also help us determine if the compounds have any direct molecular interactions with the DBL-1 pathway.

*C. elegans* exhibits immediate attraction or repulsion behaviors to different compounds including eating or not eating, and moving towards or away from stimuli (Bargmann *et al.* 1993). Avoidance behavior is considered as a protective response to adverse conditions and hence, chemotaxis assays can be used to determine preference or repulsion towards test compounds. (Ermolaeva 2014). Health and life-span are two population traits that can be used to assess the effect of a potential stressor on organisms

(Keith *et al.* 2014). Less acute toxicity can also be caused by changes in movement or development (Ingram 2000). The major goals of this study are to determine if the novel compounds have deleterious organismal effect and to determine if TGF- $\beta$ /DBL-1 signaling affects organismal responses to these potential stressors in *C. elegans*.

## Materials and Methods

### Strains and maintenance

*C. elegans* strains that were used in these studies are derived from the wild-type variety Bristol strain N2 and cultured on nematode growth media (NGM) plates as previously described (Brenner 1974). All strains were cultured on *E. coli* strain OP50 at 20°C, except where noted. Strains used include: N2, TLG182 *texIs100 [dbl-1p::dbl-1:gfp + ttx-3p::rfp]* IV (also referred to as *dbl-1(++)*); NU3 *dbl-1(nk3)* V (also referred to as *dbl-1(-)*), CB502 *sma-2(e502)* III, TLG634 *sma-3(wk30)* III, DR1369 *sma-4(e729)* III, and VC2197 *sma-6(ok2894)* II.

### Test compounds and controls

The nanocarriers were obtained from the Hynds lab, Department of Biology, Texas Woman's University and were created by the Ghosh lab, Department of Physics and Engineering Physics, Southeast Missouri State University. Compounds are named C 144, C 750 and N 150. All three have a red fluorophore attached, a type of rhodamine fluorophore B at either the N- or C- terminal end and are numbered based on diameter (in microns). Dilutions of these compounds were made with ultra-pure water and corresponding controls were ultra-pure water.



The potential anti-cancer amidoxime compounds were obtained from the Bergel lab, Department of Biology, Texas Woman's University. Amidoximes, JJMB 5 and JJMB 9 were synthesized by Dr. Debra Dolliver, Department of Chemistry and Physics, Southeast Louisiana University. Dilutions of these compounds were made with dimethylsulfoxide (DMSO) and controls were corresponding dilutions of DMSO in water.

#### Compound intake

To determine if animals ingest these fluorescent compounds, 20 wild-type *C. elegans* were picked at larval stage four (L4) onto EZ media plates spotted with compound N 150, C 144, or C 750 mixed with *E. coli* (strain OP50) food in a 1:1 ratio. Animals on the control plate were fed *E. coli* (strain OP50) food mixed with ultra-pure water in a 1:1 ratio. Animals were allowed to eat this mixture and then imaged every 24 hours up to four days. For imaging, animals were anesthetized using 1 mM levamisole hydrochloride (Sigma, St. Louis, MO) and imaged using a Nikon A1R-A1 confocal system with a Nikon Eclipse Ti inverted microscope and Nikon NIS Elements AR-3.2 imaging software (Nikon Instruments, Melville, NY). Microscopic observations were standardized to bring the fluorescence intensity values in measurable dynamic range. Animals were imaged at 60X magnification and image capturing conditions were kept constant for each experiment.

### Chemotaxis assay

To determine *C. elegans* chemotaxis in response to test compounds, chemotaxis assays were conducted as previously described (Margie *et al.* 2013). EZ media plates were divided into four quadrants (marked on the back of the plate) and spotted with 2  $\mu$ l of test compound and 2  $\mu$ l of control (water or DMSO) solutions mixed with 0.5 M of sodium azide (an anesthetic that paralyses animals) on opposing quadrants. About 100 staged young adult animals (in 2  $\mu$ l) were put on the center of the plate. The number of nematodes on each spot was scored after 1 hour. The chemotaxis index was calculated using the following formula: Chemotaxis Index = (# Worms in Both Test Quadrants - # Worms in Both Control Quadrants) / (Total # of Scored Worms). A +1.0 score indicates maximal attraction towards the target and represents 100% of the worms arriving in the quadrants containing the chemical target. An index of -1.0 signifies maximal repulsion. Chemotactic indices were generated from assays performed with wild-type, *dbl-1*(-), and *dbl-1*(++) strains using compounds N 150, C 144, and C 750 at 5%, and JJMB 5 and JJMB 9 at 0.5 mM with water and DMSO for controls. Values were averages from at least three independent experiments ( $n > 50$  animals/trial) for each condition. One-way ANOVA was used to determine significant differences between groups and Tukey's post hoc test was used to identify sample means significantly different from the control.

### Locomotion assay

Locomotion assays were conducted as previously described (Keith *et al.* 2014). Animals of each wild-type, *dbl-1*(-), and *dbl-1*(++) strain were staged and grown on potential anti-cancer and nanocarrier compounds (at concentrations 0.5mM and 5%

respectively) from embryo to L4 and approximately 100 animals of each strain had their locomotion analyzed as previously described (Keith *et al.* 2014). Specifically, the compound (or control) were mixed in a 2  $\mu$ l drop of 0.5 mM sodium azide anesthetic at the edge of an unseeded EZ media plate and its location was marked. Animals that enter the region with the compounds were immobilized. Fifty worms were placed at the center of the plate. After one hour, the locations of the worms were marked, and the mean distance covered by each strain under a particular condition was calculated. Locomotion assays were performed using compounds N 150, C 144, C 750 (5%), JJMB 5, and JJMB 9 (0.5 mM) with water and DMSO for controls. Values are averages from three independent experiments ( $n = \sim 50$  animals/trial) for each condition. A one-way ANOVA was used to determine significant differences between groups and Tukey's post hoc test was used to identify sample means significantly different from the control.

#### Body length assay

*C. elegans*, 30 animals of each wild-type, *dbl-1*(-), and *dbl-1*(++) strain were staged at L4 and the body lengths were measured as described previously (Schultz *et al.* 2014). Specifically, about 30 staged young adult animals were transferred to 2% agar pads on glass slides and were imaged when moving forward at 60X magnification using iVision-Mac software (BioVision Technologies, Exton, PA) and a Retiga-2000R CCD camera mounted on a Nikon SMZ1500 dissecting microscope. Lengths of animals were determined using the length measurement image tool within iVision-Mac software. Body lengths of the wild-type, *dbl-1*(-), and *dbl-1*(++) strains exposed to compounds N 150, C 144, C 750 (5%), JJMB 5, and JJMB 9 (0.5 mM) with water and DMSO for controls

were measured. Values are averages from three trials ( $n \sim 30$  animals/trial) for each condition. A statistical analysis was performed using the independent  $t$ -test.

### Survival assay

Survival assays were conducted as previously described (Solis and Petrascheck 2011). Wild-type, *dbl-1*(++), and *dbl-1*(-) strains were grown from larval stage one (L1) in 96-well plates containing OP50. Compounds of a range of concentrations mixed with OP50 as well as just OP50 (with water and DMSO as controls) and observed for mortality thrice a week until all the animals died. To each well, 50  $\mu\text{g}/\text{mL}$  Carbenicillin, 0.1  $\mu\text{g}/\text{mL}$  Amphotericin B, and 0.6 mM FUDR were also added. Compounds N 150, C 144, and C 750 were tested at concentrations 1%, 2.5% and 5%. Compounds JJMB 5 and JJMB 9 were tested at concentrations 1  $\mu\text{M}$ , 10  $\mu\text{M}$ , 0.1 mM, and 0.5 mM. For each of the conditions,  $n = \sim 30$ . Controls of water, OP50, and DMSO were used in appropriate corresponding concentrations. The survival assay was done in triplicates. Survival analyses were illustrated on Kaplan-Meier plots using SPSS and statistical analyses conducted using the log-rank test.

### Results

#### Fluorescent test compounds are ingested by *C. elegans*

To determine if fluorescent nanocarriers N 150, C 144, and C 750 are ingested by animals, we picked wild-type strains at larval stage four (L4) on plates with or without 1.5% compound and observed animals daily for four days using confocal microscopy. We observed red fluorescence initially at the oral opening on Day 1 in the animals exposed to the compounds. Whereas there was no red fluorescence observed in the

control nematodes. The red fluorescent compounds progressed from the oral opening, through the pharynx, intestine, and all the way to the anus by Day 4 (N 150 not shown in figure) (see Figure 3.1). All these compounds progressed through the intestinal tract at a similar rate. The fluorescence does not fade in the acidic environment of the gut. After the fluorescence could be seen through from the mouth to the anus of the animal, the animals were transferred to a plate that did not contain any compound to observe if the animals could successfully clear out the compound from their body. We observed that after 4 hours, there was complete clearance of the compound as no fluorescence could be seen beyond that point.

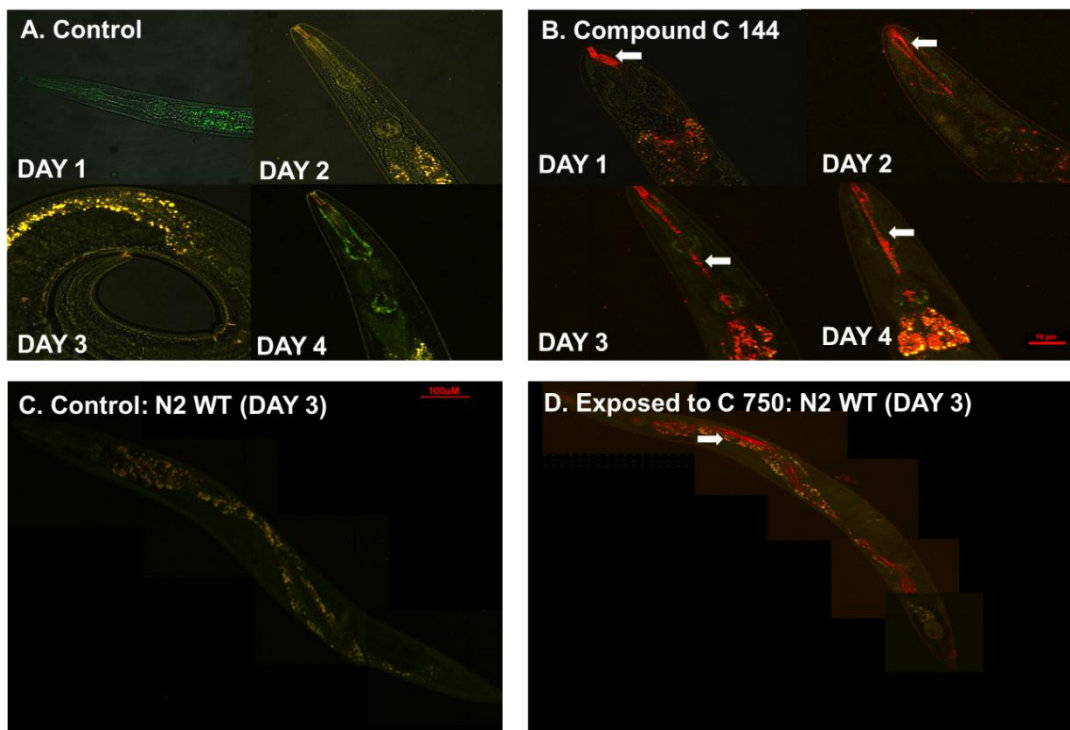


Figure 3.1. Fluorescent compounds are ingested but not degraded in *C. elegans*. A. Wild-type animals on *E. coli* plates over a period of 4 days. B. Wild-type animals on *E. coli* mixed with 1.5% compound C 144 over 4 days. C. Wild-type animals on *E. coli* at Day 3. D. Wild-type animals on compound C 750 at Day 3. Arrows note red fluorescence of the compound.

These results confirm that the worms can consume the fluorescent test compounds when supplied to them mixed with their primary food source, *E. coli*, at 1.5% concentration. As fluorescence is observed only in the intestinal lumen and not inside cells or elsewhere in the body, we confirmed that the compounds do not diffuse through the cell walls of the intestine or the cuticle. Furthermore, compounds are not degraded over the tested period in the intestinal lumen and are able to be cleared out of the animal.

Test compounds exhibit a positive chemotaxis to the compounds

To investigate if these compounds elicit attraction or repulsion responses and to test for involvement of DBL-1 signaling in this behavior, wild-type, *dbl-1*(-), and *dbl-1*(++) L4 animals were exposed to the fluorescent test compounds N 150, C 144, and C 750 (5% concentration) and JJMB 5 and JJMB 9 (0.5 mM). Wild-type worms exhibited a significantly greater attraction towards compounds C 144 and C 750 compared to the control ( $p < 0.05$ ). *dbl-1*(-) worms exhibited a significantly greater attraction towards all the three fluorescent test compounds ( $p < 0.05$ ) (see Figure 3.2). *dbl-1*(++) worms exhibited a significantly greater attraction towards compounds N 150 and C 144 as compared to the control ( $p < 0.05$ ) (see Figure 3.2). For the amidoximes, we observed that *dbl-1*(-) and *dbl-1*(++) worms exhibited a significantly reduced yet positive attraction towards both JJMB 5 and JJMB 9 as compared to the controls ( $p < 0.05$ ) (see Figure 3.2). None of the strains exhibited repulsion behavior towards any compound. Absence or overexpression of DBL-1 does not cause any repulsive behavior. These results give evidence that these compounds do not elicit aversion behavior and altering

DBL-1 signaling does not sensitize animals to these compounds to increase negative responses.

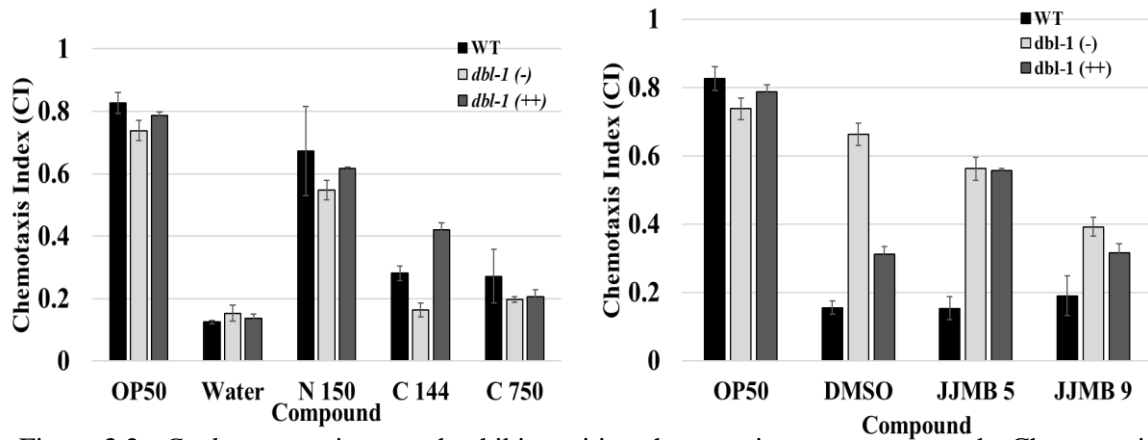


Figure 3.2. *C. elegans* strains tested exhibit positive chemotaxis to test compounds. Chemotactic indices generated from assays performed with wild-type, *dbl-1*(-), and *dbl-1*(++) strains using A. compounds N 150, C 144, C 750 (5%), compared with water as Control 1, and B. Compounds JJMB 5 and JJMB 9 (0.5 mM) compared with DMSO as Control 2. Values are averages from at least three independent experiments ( $n > 50$  animals/trial) for each condition. Error bars reflect the standard deviation (SD). \* =  $p < 0.05$  by ANOVA.

#### Test compounds do not affect motility

Milder effects may be seen in degeneration over time. Mobility assays are used to determine deterioration caused by the compound or mutation of interest (Keith *et al.* 2014). To investigate the movement coordination of the animals exposed to the test compounds and to test for involvement of DBL-1 signaling, wild-type, *dbl-1*(-), and *dbl-1*(++) strains at larval stage four (L4) were exposed to the test compounds N 150, C 144, and C 750 (5% concentration) and non-fluorescent test compounds JJMB 5 and JJMB 9 (0.5 mM) for one hour. Animals were observed when and how? No significant differences in locomotion were observed for any of the compounds as compared to controls in any of the tested strains (see Figure 3.3). The genetic background did not affect locomotion or make animals more sensitive or resistant on controls or tested

compounds. These results suggest that the test compounds do not affect the locomotion of the animals.

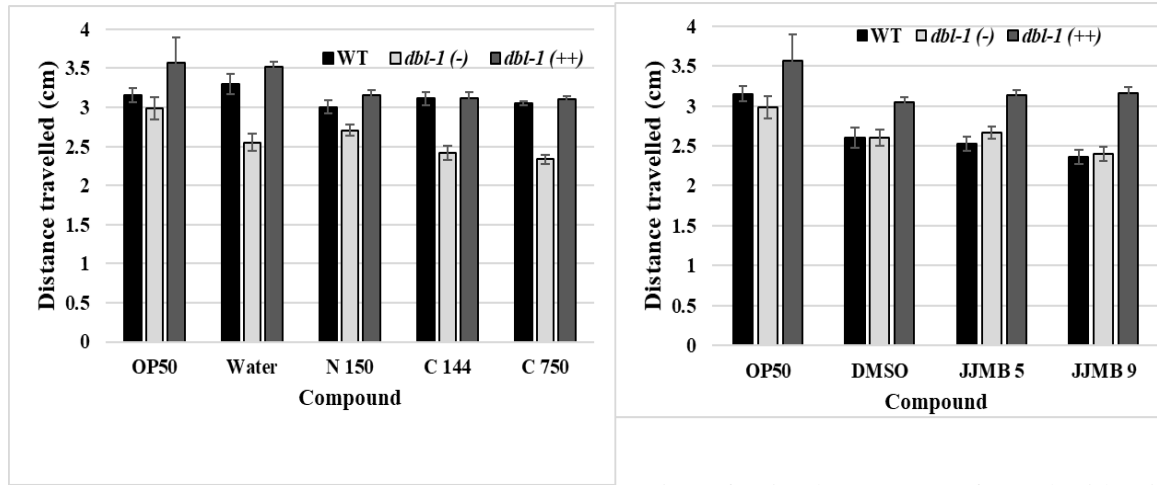


Figure 3.3. Test compounds do not affect locomotion of animals. Assay performed with wild-type, *dbl-1*(-), and *dbl-1*(++) strains using A. compounds N 150, C 144, C 750 (5%), with water as Control 1, B. JJMB 5, and JJMB 9 (0.5 mM) with DMSO as Control 2. Values are averages from two independent experiments ( $n \approx 50$  animals/trial) for each condition. Error bars reflect the standard error of mean (SEM). The ANOVA was used for statistical analysis.

Test compounds do not affect body length

Mild effects can be revealed in developmental effects, especially in body size. To investigate the effect of test compounds on body length and to test for involvement of DBL-1 signaling, wild-type, *dbl-1*(-), and *dbl-1*(++) strains at larval stage four (L4) were exposed to the test compounds N 150, C 144, and C 750 (5% concentration) and JJMB 5 and JJMB 9 (0.5 mM). No significant differences in body length were observed for any of the compounds as compared to controls in any of the tested strains (see Table 3.1). These results suggest that the tested compounds do not affect the body length of the animals in DBL-1 dependent or independent ways.



	<b>WT</b>	<i>dbl-1</i> (-)	<i>dbl-1</i> (++)
<b>Water</b>	100±4	100±4	100±3
<b>N 150</b>	102±4	103±4	98±2
<b>C 144</b>	100±3	103±3	100±3
<b>C 750</b>	100±3	103±4	98±2
<b>DMSO</b>	100±3	100±3	100±2
<b>JJMB 5</b>	100±4	98±3	98±2
<b>JJMB 9</b>	102±3	96±4	99±2

Table 3.1. Test compounds do not alter body length of animals. Body lengths of the wild-type, *dbl-1*(-), and *dbl-1*(++) strains exposed to compounds N 150, C 144, C 750 (5%), JJMB 5, and JJMB 9 (0.5 mM) with water (Control 1) and DMSO (Control 2) for controls were measured. Values are normalized to controls ( $n=30$  animals/trial). The unpaired *t*-test was used for statistical analysis.

#### Test compounds do not affect survival

Lifespan assays are used to determine if compound or mutation of interest affects age-related deterioration (Keith *et al.* 2014). To investigate the effect of the test compounds on lifespan of *C. elegans*, we tested compounds N 150, C 144, and C 750 at 1%, 2.5%, and 5%. Compounds JJMB 5 and JJMB 9 were tested at 1  $\mu$ M, 10  $\mu$ M, 100  $\mu$ M, and 500  $\mu$ M. We used wild-type and DBL-1 pathway mutant strains *dbl-1*(-), *dbl-1*(++), *sma-2*(-), *sma-3*(-), and *sma-6*(-) to determine if the canonical or non-canonical DBL-1 pathway was involved in generating a stress response, if any. For each of the conditions,  $n = \sim 30$ .

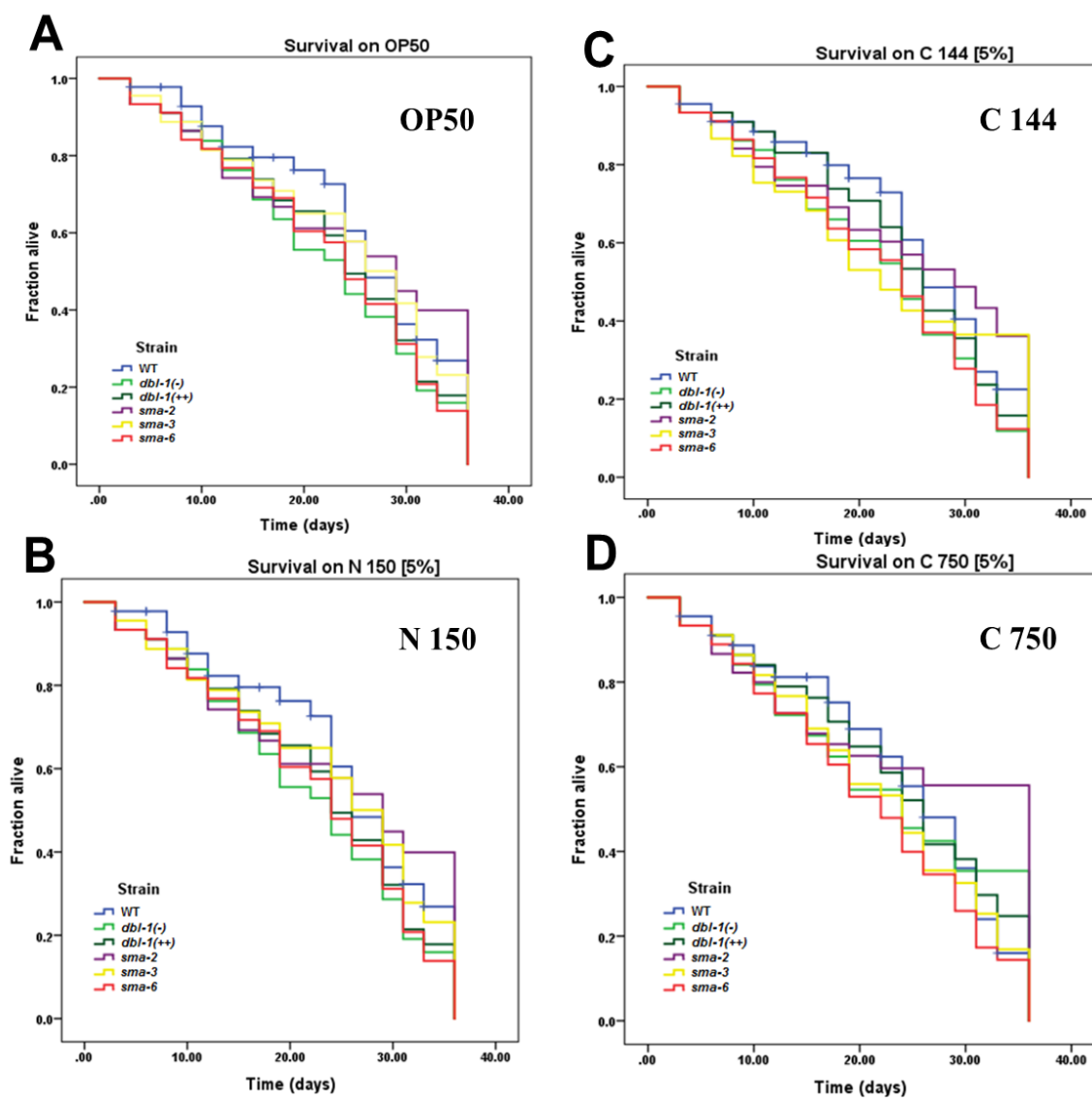


Figure 3.4. Survival of animals was not affected by test compounds. Survival curves of different strains over a period of 36 days grown in different concentrations of compound. A-D. Survival curves of wild-type (blue), *dbl-1(-)* (green), *dbl-1(+++)* (dark blue), *sma-2* (purple), *sma-3* (yellow), and *sma-6* (red) populations on OP50 and compounds N 150, C 144, and C 750 (5%).

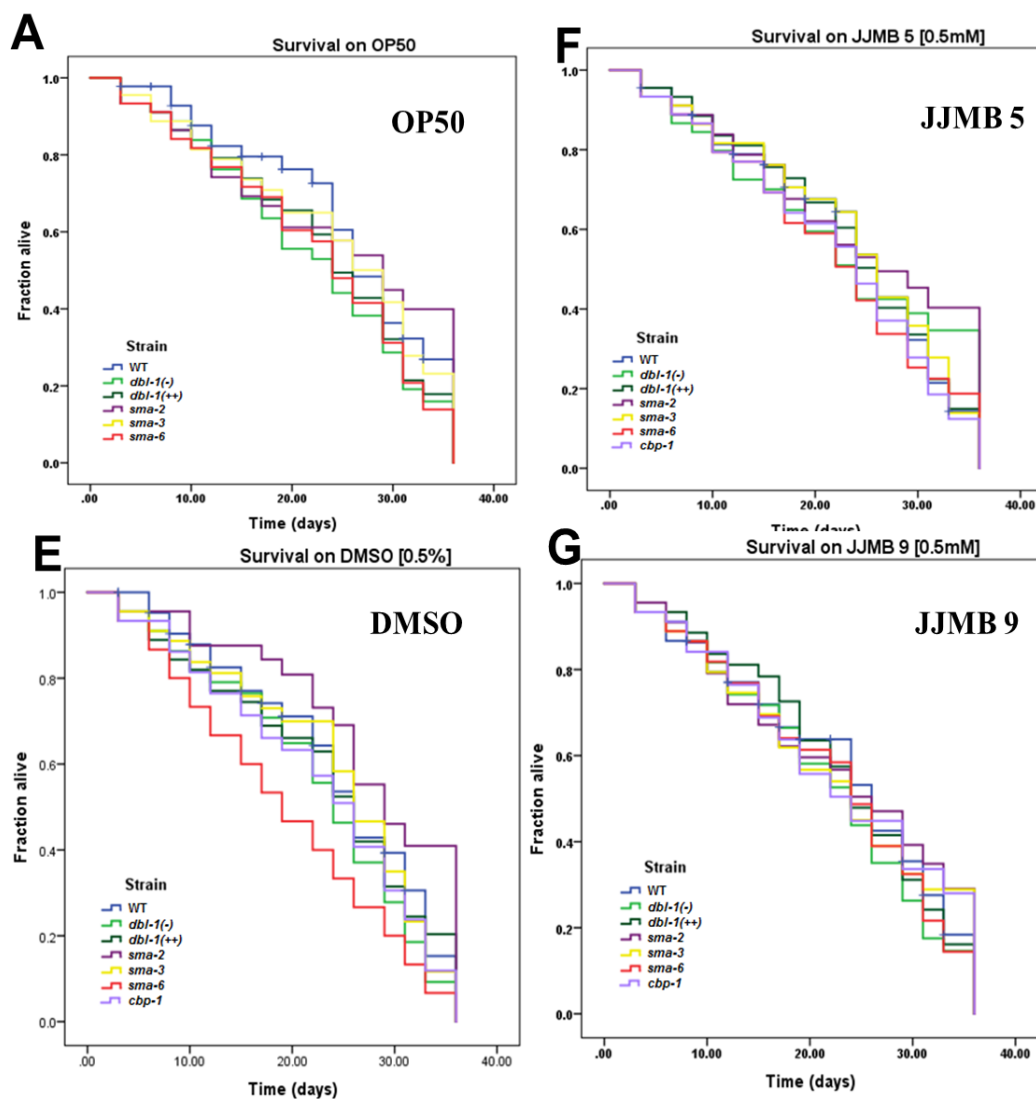


Figure 3.4. (continued) Survival of animals was not affected by test compounds. Survival curves of different strains over a period of 36 days in different concentrations of compound. A Shows the survival of type (blue), *dbl-1(-)* (green), *dbl-1(+++)* (dark blue), *sma-2* (purple), *sma-3* (yellow), and *sma-6* (red) populations on OP50. E-G. Survival curves of the same strains on DMSO (0.5% concentration) and JJMB 5 and JJMB 9 (0.5 mM). For each of the conditions,  $n \sim 15$  animals/trial.

Controls of water, OP50, and DMSO were used in appropriate corresponding concentrations. We scored worms populations until all the test animals died. We generated Kaplan-Meier survival plots using SPSS software. No significant differences in survival of the worms exposed to different test compounds at varying concentrations as compared to corresponding controls was observed as calculated by log rank test using SPSS ( $p > 0.05$ ). The results using the highest tested concentration are shown (see Figure 3.4). Animals on control versus test compounds did not exhibit a significantly different mortality at the tested concentrations. Changes in DBL-1 signaling do not affect life-span or how populations respond to the tested nanocarriers and amidoximes.

## Discussion

*C. elegans* has been established as a model for toxicity testing to predict toxicity ranking in mammals (Hunt 2017). The simplest method of delivering a substance to the worm is through its food. The first step of digestion is at the pharyngeal grinder, and then lysozymes, saponins etc., cause breakdown of food material (Mcghee 2007). Since we could see our test compounds from the mouth to the anus, it is unlikely that there is any significant breakdown of the compounds tested. The gut lumen is known to be mildly acidic, however, it did not appear to cause any damage to the fluorescent test compounds' integrity.

*C. elegans* exhibits attraction or repulsion to different compounds based on the chemical cues it receives (Bargmann *et al.* 1993). Avoidance behavior is considered an

immune response because it triggers the same response following a protective learning experience against an aversive substance (Ermolaeva 2014; Meisel and Kim 2014). Because we introduced the test compounds to the animals orally, it is essential that the worms do not perceive the test compounds as a threat or repellant and avoid it. The *dbl-1* mutant strains showed an increased attraction towards the fluorescent test compounds as compared to the control. However, the *dbl-1* mutant strains showed a decreased attraction towards the non-fluorescent test compounds as compared to the control. This suggests that there might be differences in perception based on differences between compounds. These results do not clearly indicate a role for DBL-1 signaling in response to these compounds. Overall, the animals exhibit a positive chemotaxis, suggesting the compounds do not generate a negative stress response in the animals. Thus, the compounds at the tested concentration can be considered safe enough to be tested in mammalian systems.

Coordinated movement is an important characteristic of wild-type *C. elegans* that indicates its health (Keith *et al.* 2014). Drug-like compounds can disrupt the locomotion of animals (Holden-Dye and Walker 2014). Our results show lack of significant differences in mobility between exposure to control and test compounds at varying concentrations in all the tested strains. Lack of significant differences in motility between wild-type and DBL-1 mutants suggests that alteration of this pathway does not sensitize animals to possible deleterious effects of the tested compounds at the concentrations tested. However, the tested concentrations of the various compounds might not have been high enough to elicit a stress response.

Wild-type body length is an indicator of proper development and health in *C. elegans*. DBL-1 is known to regulate body length in a dose-dependent manner (Schultz *et al.* 2014). Our results show lack of significant differences in body length between exposure to control and test compounds at varying concentrations in all the tested strains. Lack of significant differences in body length between wild-type and DBL-1 mutants suggests a lack of involvement of DBL-1 signaling pathway in generating a stress response to the test compounds. However, the tested concentrations of the various compounds might not have been high enough to elicit a stress response.

Studying the lifespan of our model organism helps us elucidate the effect of test compounds on mortality and/or the aging process (Park 2017). Our results show lack of significant differences in lifespan between exposure to control and test compounds at varying concentrations in all the tested strains. Lack of significant differences in lifespan between wild-type and DBL-1 pathway mutants exposed to different concentrations of the test compounds suggests a lack of involvement of DBL-1 signaling pathway in generating a stress response to these specific compounds. However, the tested concentrations of the various compounds might not have been high enough to elicit a stress response to these compounds.

DBL-1 signaling mutants do not have altered motility or life-span caused by test compounds. Also, alteration of this pathway does not sensitize animals to possible deleterious effects of the tested compounds. The multiple aspects of testing support the conclusion that the tested concentrations of the three nanocarriers and two amidoximes may be considered safe to be tested in mammalian systems.

## CHAPTER IV

### CONCLUSIONS AND FUTURE DIRECTIONS

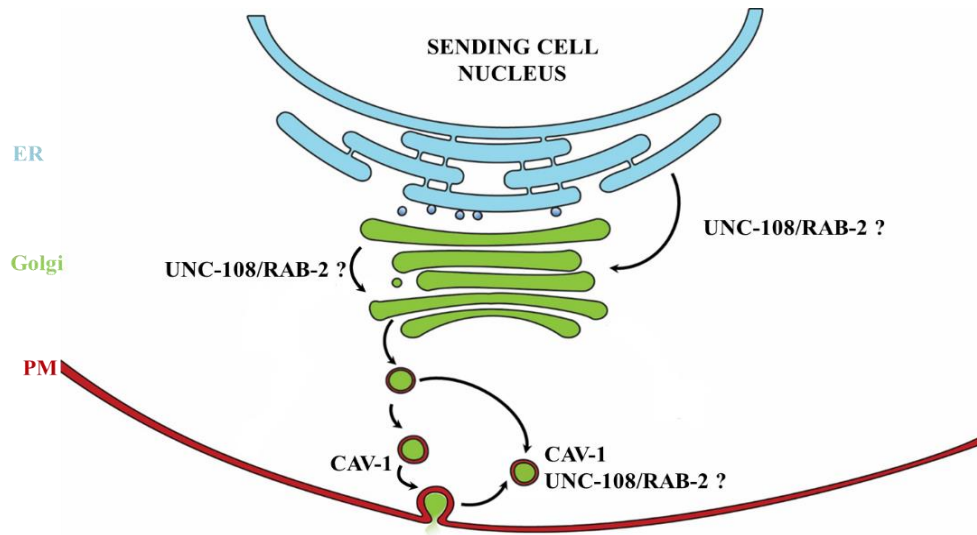


Figure 4.1. Model TGF- $\beta$ /DBL-1 trafficking in *C. elegans*. Nascent DBL-1 (bright green) is trafficked from ER to Golgi with the assistance of UNC-108/RAB-2. DBL-1 is trafficked from the Golgi to the plasma membrane with CAV-1/caveolin along microtubules. DBL-1 secretion is regulated by CAV-1 in a “kiss-and-run” membrane fusion. Adapted from De Matteis and Luini (2011).

The TGF- $\beta$  superfamily of ligands regulates a myriad of developmental programs. In humans, misregulation of TGF- $\beta$  signaling results in a variety of developmental disorders, including pathologies associated with the cardiovascular and skeletal systems, as well as numerous cancers (Moustakas and Heldin 2009a). Because of the adverse consequences of aberrant signaling, it is of great importance to characterize the regulation of TGF- $\beta$  signal transduction. Using the genetic model organism *C. elegans*, we have elucidated some regulatory mechanisms and responses related to TGF- $\beta$  signaling.

Because there is a high level of conservation between the TGF- $\beta$  transduction pathways across metazoans, the insights gained from work in this organism may lead to a better understanding of TGF- $\beta$  signaling in general (Lai *et al.* 2000). The focus of the studies described in this thesis is to elucidate the localization of DBL-1, regulation of DBL-1 at the level of the sending cell, the effect of DBL-1 on surface barrier composition (Chapter II), and the role of DBL-1 in toxicity responses to drug/drug-carrier compounds (Chapter III).

We discovered that *dbl-1* is expressed in a different pattern than previously published (see Figure 1.1). This expanded DBL-1 expression pattern may help us understand how cells that secrete DBL-1 receive regulatory cues from environmental sensing or other neurons. We determined that CAV-1 and UNC-108 are regulators of TGF- $\beta$ /DBL-1 trafficking (see Figure 4.1). This clarifies the trafficking pathway for DBL-1 secretion, and also identifies new roles for both CAV-1 and UNC-108 in regulating DBL-1 trafficking. BEC-1, an autophagy gene required for normal body size, does not co-localize with DBL-1, suggesting that BEC-1's role in body size is not through direct regulation of DBL-1 trafficking (Aladzsiy *et al.* 2007). Identifying the regulators of TGF- $\beta$ /DBL-1 trafficking may aid in the understanding of disorders that arise as a result of misregulated TGF- $\beta$  signaling, facilitating the discovery of new therapeutics for TGF- $\beta$  pathway-based diseases that currently do not respond well to conventional therapies.

We also studied the effects of this pathway on the roundworm's epicuticle, a protective barrier that covers this animal and is the first line of defense against infection,



many drugs, and other potentially damaging agents in its environment (Edgar *et al.* 1982; Sifri *et al.* 2005; Page and Johnstone 2007). We established that there are differences in lipid composition between wild-type and TGF- $\beta$ /DBL-1 pathway mutant epicuticles. Exploiting this information, we can identify the lipids themselves and genes that synthesize significant surface lipids to act as drug targets. Weakened epicuticle could increase permeability of cuticle and compromise worms' survival by making animals more susceptible to environmental stressors and anthelmintic drugs.

The knowledge of how drug or drug-carrier compounds affect the body will facilitate the choice of drugs to continue through the expensive, time-consuming drug development pipeline (Hughes *et al.* 2011). We established that three nanocarrier compounds, N 150, C 144, and C 750, and two potential anti-cancer drug compounds, JJMB 5 and JJMB 9, do not induce a toxicity response in *C. elegans* (Chapter III). Furthermore, alterations that increase or decrease DBL-1 signaling do not sensitize animals to these compounds. Therefore, the DBL-1 pathway does not affect the responses to the tested compounds at the tested concentrations. In addition, our results provide justification for testing the compounds in higher organisms. Further studies in mammalian systems will provide further evidence for the feasibility of drug safety testing in humans.

The ultimate goal is to obtain an integrated molecular model for molecular, cellular, and organismal responses mediated by TGF- $\beta$ /DBL-1 signaling pathway in our model organism, *C. elegans*, in response to environmental stressors, which may be

translated to higher organisms, including humans. This work provides essential stepping stones to achieve this goal.

## CHAPTER V

### REFERENCES

- Aladzsity, I., M. L. Toth, T. Sigmond, E. Szabo, B. Bicsak et al., 2007. Autophagy genes *unc-51* and *bec-1* are required for normal cell size in *Caenorhabditis elegans*. Genetics 177: 655-660.
- Altun, Z. F., and D. H. Hall, 2011. Nervous system, general description. WormAtlas.
- Bae, Y. K., J. Y. Sung, Y. N. Kim, S. Kim, K. M. Hong et al., 2012. An *in vivo* *C. elegans* model system for screening EGFR-inhibiting anti-cancer drugs. PLoS One 7: e42441.
- Bargmann, C. I., 2001. High-throughput reverse genetics: RNAi screens in *Caenorhabditis elegans*. Genome Biol 2: reviews1005.1001-1003.
- Bargmann, C. I., E. Hartwig and H. R. Horvitz, 1993. Odorant-selective genes and neurons mediate olfaction in *C. elegans*. Cell 74: 515-527.
- Beifuss, K. K., and T. L. Gumienny, 2012. RNAi screening to identify postembryonic phenotypes in *C. elegans*. J Vis Exp: e3442.
- Blobe, G. C., W. P. Schiemann and H. F. Lodish, 2000. Role of transforming growth factor beta in human disease. N Engl J Med 342: 1350-1

- Boyd, W. A., M. V. Smith and J. H. Freedman, 2012. *Caenorhabditis elegans* as a model in developmental toxicology. *Methods Mol Biol* 889: 15-24.
- Brenner, S., 1974. The genetics of *Caenorhabditis elegans*. *Genetics* 77: 71-94.
- Candido, E. P., and D. Jones, 1996. Transgenic *Caenorhabditis elegans* strains as biosensors. *Trends Biotechnol* 14: 125-129.
- Charoenphol, P., and H. Bermudez, 2014. Design and application of multifunctional DNA nanocarriers for therapeutic delivery. *Acta Biomater* 10: 1683-1691.
- Chen, Y. G., A. Hata, R. S. Lo, D. Wotton, Y. Shi et al., 1998. Determinants of specificity in TGF- $\beta$  signal transduction. *Genes Dev* 12: 2144-2152.
- Cheung, A. Y., C. Y. Chen, R. H. Glaven, B. H. J. de Graaf, L. Vidali et al., 2002. Rab2 GTPase regulates vesicle trafficking between the endoplasmic reticulum and the Golgi bodies and is important to pollen tube growth. *Plant Cell* 14: 945-962.
- Chun, D. K., J. M. McEwen, M. Burbea and J. M. Kaplan, 2008. UNC-108/Rab2 regulates postendocytic trafficking in *Caenorhabditis elegans*. *Mol Biol Cell* 19: 2682-2695.
- Corsi, A. K., B. Wightman and M. Chalfie, 2015. A transparent window into biology: A primer on *Caenorhabditis elegans*. 200: 387-407.
- Daugherty, C. E., and H. G. Lento, 1983. Chloroform-methanol extraction method for determination of fat in foods: collaborative study. *J Assoc Off Anal Chem* 66: 927-932

- Derynck, R., and Y. E. Zhang, 2003. Smad-dependent and Smad-independent pathways in TGF- $\beta$  family signalling. *Nature* 425: 577-584.
- Dillin, A., D. K. Crawford and C. Kenyon, 2002. Timing requirements for insulin/IGF-1 signaling in *C. elegans*. *Science* 298: 830-834.
- Donkin, S. G., M. A. Eiteman and P. L. Williams, 1995. Toxicity of glucosinolates and their enzymatic decomposition products to *Caenorhabditis elegans*. *J Nematol* 27: 258-262.
- Ermolaeva, M. A., 2014. Insights from the worm: The *C. elegans* model for innate immunity. 26: 303-309.
- Feng, X. H., and R. Derynck, 2005. Specificity and versatility in TGF- $\beta$  signaling through Smads. *Annu Rev Cell Dev Biol* 21: 659-693.
- Fernando, T., S. Flibotte, S. Xiong, J. Yin, E. Yzeiraj et al., 2011. *C. elegans* ADAMTS ADT-2 regulates body size by modulating TGF $\beta$  signaling and cuticle collagen organization. *Dev Biol* 352: 92-103.
- Fire, A., S. Xu, M. K. Montgomery, S. A. Kostas, S. E. Driver et al., 1998. Potent and specific genetic interference by double-stranded RNA in *Caenorhabditis elegans*. *Nature* 391: 806-811.
- Flemming, A. J., Z. Z. Shen, A. Cunha, S. W. Emmons and A. M. Leroi, 2000. Somatic polyploidization and cellular proliferation drive body size evolution in nematodes. *Proc Natl Acad Sci U S A* 97: 5285-5290.

- Flora, K. P., B. Van't Riet and G. L. Wampler, 1978. Antitumor activity of amidoximes (hydroxyurea analogs) in murine tumor systems. *Cancer Res* 38: 1291-1295.
- Fulda, S., A. M. Gorman, O. Hori and A. Samali, 2010. Cellular stress responses: Cell survival and cell death. *International Journal of Cell Biology* 2010: 23.
- Gallegos, M. E., S. Balakrishnan, P. Chandramouli, S. Arora, A. Azameera et al., 2012. The *C. elegans rab* family: identification, classification and toolkit construction. *PLoS One* 7: e49387.
- Ghosh, S., S. Ghoshmitra, T. Cai, D. R. Diercks, N. C. Mills et al., 2009. Alternating magnetic field controlled, multifunctional nano-reservoirs: Intracellular uptake and improved biocompatibility. *Nanoscale Res Lett* 5: 195-204.
- GhoshMitra, S., D. R. Diercks, N. C. Mills, D. A. L. Hynds and S. Ghosh, 2013. Moderate level exposure to magnetic nanodots encased in tunable poly(ethylene glycol) analogue biopolymer shell do not deleteriously affect neurite outgrowth. *Journal of Nanoscience and Nanotechnology* 13: 8290-8297.
- GhoshMitra, S., D. R. Diercks, N. C. Mills, D. L. Hynds and S. Ghosh, 2011. Excellent biocompatibility of semiconductor quantum dots encased in multifunctional poly(N-isopropylacrylamide) nanoreservoirs and nuclear specific labeling of growing neurons. *Applied Physics Letters* 98: 103702.

- GhoshMitra, S., D. R. Diercks, N. C. Mills, D. L. Hynds and S. Ghosh, 2012. Role of engineered nanocarriers for axon regeneration and guidance: current status and future trends. *Adv Drug Deliv Rev* 64: 110-125.
- GhoshMitra, S., T. Cai, D. Diercks, Z. Hu, J. Roberts et al., 2011. Evaluation of the biological effects of externally tunable, hydrogel encapsulated quantum dot nanospheres in *Escherichia coli*. *Polymers* 3: 1243-1254.
- Golden, A., 2009. Inactivation of the *C. elegans* lipin homolog leads to ER. 122: 1970-1978.
- Groppe, J., C. S. Hinck, P. Samavarchi-Tehrani, C. Zubieta, J. P. Schuermann et al., 2008. Cooperative assembly of TGF-beta superfamily signaling complexes is mediated by two disparate mechanisms and distinct modes of receptor binding. *Mol Cell* 29: 157-168.
- Gumienny, T. L., and C. Savage-Dunn, 2013. TGF- $\beta$  signaling in *C. elegans*, in *WormBook*, edited by The *C. elegans* Research Community. *WormBook*: 1-34.
- Gumienny, T. L., L. Macneil, C. M. Zimmerman, H. Wang, L. Chin et al., 2010. *Caenorhabditis elegans* SMA-10/LRIG is a conserved transmembrane protein that enhances bone morphogenetic protein signaling. *PLoS Genet* 6: e1000963.
- Gumienny, T. L., L. T. MacNeil, H. Wang, M. de Bono, J. L. Wrana et al., 2007. Glypican LON-2 is a conserved negative regulator of BMP-like signaling in *Caenorhabditis elegans*. *Curr Biol* 17: 159-164.

- Guo, X., and X. F. Wang, 2009. Signaling cross-talk between TGF- $\beta$ /BMP and other pathways. *Cell Res* 19: 71-88.
- Heiman, M. G., and S. Shaham, 2009. DEX-1 and DYF-7 establish sensory dendrite length by anchoring dendritic tips during cell migration. *Cell* 137: 344-355.
- Hilliard, M. A., A. J. Apicella, R. Kerr, H. Suzuki, P. Bazzicalupo et al., 2005. *In vivo* imaging of *C. elegans* ASH neurons: cellular response and adaptation to chemical repellents. *Embo j* 24: 63-72.
- Hodgkin, J., M. A. Felix, L. C. Clark, D. Stroud and M. J. Gravato-Nobre, 2013. Two *Leucobacter* strains exert complementary virulence on *Caenorhabditis* including death by worm-star formation. *Curr Biol* 23: 2157-2161.
- Holden-Dye, L., and R. J. Walker, 2014. Anthelmintic drugs and nematicides: studies in *Caenorhabditis elegans*, in *WormBook*, edited by The *C. elegans* Research Community. *WormBook*: 1-29.
- Huang, K. T., C. T. Wu, K. H. Huang, W. C. Lin, C. M. Chen et al., 2015. Titanium nanoparticle inhalation induces renal fibrosis in mice via an oxidative stress upregulated transforming growth factor- $\beta$  pathway. *Chem Res Toxicol* 28: 354-364.
- Hunt, P. R., 2017. The *C. elegans* model in toxicity testing. *J Appl Toxicol* 37: 50-59.
- Ingram, D. K., 2000. Age-related decline in physical activity: generalization to nonhumans. *Med Sci Sports Exerc* 32: 1623-1629.



- Kagias, K., C. Nehammer and R. Pocock, 2012. Neuronal responses to physiological stress. *Front Genet* 3.
- Kaletta, T., and M. O. Hengartner, 2006. Finding function in novel targets: *C. elegans* as a model organism. *Nat Rev Drug Discov* 5: 387-398.
- Kang, Y., C. R. Chen and J. Massague, 2003. A self-enabling TGF- $\beta$  response coupled to stress signaling: Smad engages stress response factor ATF3 for Id1 repression in epithelial cells. *Mol Cell* 11: 915-926.
- Kaplan, R. E., Y. Chen, B. T. Moore, J. M. Jordan, C. S. Maxwell et al., 2015. *dbl-1*/TGF- $\beta$  and *daf-12*/NHR signaling mediate cell-nonautonomous effects of daf-16/FOXO on starvation-induced developmental arrest. *PLoS Genet* 11: e1005731.
- Kassahn, K. S., R. H. Crozier, H. O. Portner and M. J. Caley, 2009. Animal performance and stress: responses and tolerance limits at different levels of biological organisation. *Biol Rev Camb Philos Soc* 84: 277-292.
- Keith, S. A., F. R. Amrit, R. Ratnappan and A. Ghazi, 2014. The *C. elegans* healthspan and stress-resistance assay toolkit. *Methods* 68: 476-486.
- Kobet, R. A., X. Pan, B. Zhang, S. C. Pak, A. S. Asch et al., 2014. *Caenorhabditis elegans*: A model system for anti-cancer drug discovery and therapeutic target identification. *Biomol Ther (Seoul)* 22: 371-383.

- Krishna, S., L. L. Maduzia and R. W. Padgett, 1999. Specificity of TGF $\beta$  signaling is conferred by distinct type I receptors and their associated SMAD proteins in *Caenorhabditis elegans*. *Development* 126: 251-260.
- Kyriakakis, E., M. Markaki and N. Tavernarakis, 2015. *Caenorhabditis elegans* as a model for cancer research. *Mol Cell Oncol* 2: e975027.
- Lai, C. H., C. Y. Chou, L. Y. Ch'ang, C. S. Liu and W. Lin, 2000. Identification of novel human genes evolutionarily conserved in *Caenorhabditis elegans* by comparative proteomics. *Genome Res* 10: 703-713.
- Lee, R. Y., J. Hench and G. Ruvkun, 2001. Regulation of *C. elegans* DAF-16 and its human ortholog FKHL1 by the *daf-2* insulin-like signaling pathway. *Curr Biol* 11: 1950-1957.
- Leung, M. C. K., P. L. Williams, A. Benedetto, C. Au, K. J. Helmcke et al., 2008. *Caenorhabditis elegans*: An emerging model in biomedical and environmental toxicology. *Toxicol Sci* 106: 5-28.
- Mallo, G. V., C. L. Kurz, C. Couillault, N. Pujol, S. Granjeaud et al., 2002. Inducible antibacterial defense system in *C. elegans*. *Curr Biol* 12: 1209-1214.
- Mangahas, P. M., 2008. The small GTPase Rab2 functions in the removal of apoptotic cells in *Caenorhabditis elegans*. 180: 357-373.
- Margie, O., C. Palmer and I. Chin-Sang, 2013. *C. elegans* chemotaxis assay. *J Vis Exp*: e50069.

- McGhee, J. D., 2007. The *C. elegans* intestine, in WormBook, edited by The *C. elegans* Research Community. WormBook.
- Meisel, J. D., and D. H. Kim, 2014. Behavioral avoidance of pathogenic bacteria by *Caenorhabditis elegans*. Trends Immunol 35: 465-470.
- Meulmeester, E., and P. Ten Dijke, 2011. The dynamic roles of TGF- $\beta$  in cancer. J Pathol 223: 205-218.
- Morita, K., K. L. Chow and N. Ueno, 1999. Regulation of body length and male tail ray pattern formation of *Caenorhabditis elegans* by a member of TGF- $\beta$  family. Development 126: 1337-1347.
- Moustakas, A., and C. H. Heldin, 2009. The regulation of TGF $\beta$  signal transduction. Development 136: 3699-3714.
- Nagamatsu, Y., and Y. Ohshima, 2004. Mechanisms for the control of body size by a G-kinase and a downstream TGF $\beta$  signal pathway in *Caenorhabditis elegans*. Genes to Cells 9: 39-47.
- Padua, D., and J. Massague, 2009. Roles of TGF $\beta$  in metastasis. Cell Res 19: 89-102.
- Page, A. P., and I. L. Johnstone, 2007. The cuticle, in WormBook, edited by The *C. elegans* Research Community. WormBook.
- Parasuraman, S., 2011. Toxicological screening. J Pharmacol Pharmacother 2: 74-79.
- Park, H. E. H., 2017. Survival assays using *Caenorhabditis elegans*. 40: 90-99.

- Park, S. H., S. R. Lee, B. C. Kim, E. A. Cho, S. P. Patel et al., 2002. Transcriptional regulation of the transforming growth factor beta type II receptor gene by histone acetyltransferase and deacetylase is mediated by NF-Y in human breast cancer cells. *J Biol Chem* 277: 5168-5174.
- Parkar, N. S., B. S. Akpa, L. C. Nitsche, L. E. Wedgewood, A. T. Place et al., 2009. Vesicle formation and endocytosis: Function, machinery, mechanisms, and modeling. *Antioxid Redox Signal* 11: 1301-1312.
- Patel, H. H., 2009. Lipid rafts and caveolae and their role in compartmentation of redox. 11: 1357-1372.
- Patterson, G. I., and R. W. Padgett, 2000. TGF  $\beta$ -related pathways. Roles in *Caenorhabditis elegans* development. *Trends Genet* 16: 27-33.
- Pelkmans, L., 2005. Secrets of caveolae- and lipid raft-mediated endocytosis revealed by mammalian viruses. *Biochim Biophys Acta* 1746: 295-304.
- Poniatowski Ł, A., P. Wojdasiewicz, R. Gasik and D. Szukiewicz, 2015. Transforming growth factor beta family: Insight into the role of growth factors in regulation of fracture healing biology and potential clinical applications. *Mediators Inflamm* 2015.
- Roberts, A. F., T. L. Gumienny, R. J. Gleason, H. Wang and R. W. Padgett, 2010. Regulation of genes affecting body size and innate immunity by the DBL-1/BMP-like pathway in *Caenorhabditis elegans*. *BMC Dev Biol* 10: 61.

- Rodriguez, M., L. B. Snoek, M. De Bono and J. E. Kammenga, 2013. Worms under stress: *C. elegans* stress response and its relevance to complex human disease and aging. *Trends Genet* 29: 367-374.
- Ruck, A., J. Attonito, K. T. Garces, L. Nunez, N. J. Palmisano et al., 2011. The Atg6/Vps30/Beclin 1 ortholog BEC-1 mediates endocytic retrograde transport in addition to autophagy in *C. elegans*. *Autophagy* 7: 386-400.
- Salleh, M. R., 2008. Life event, stress and illness. *Malays J Med Sci* 15: 9-18.
- Sambongi, Y., T. Nagae, Y. Liu, T. Yoshimizu, K. Takeda et al., 1999. Sensing of cadmium and copper ions by externally exposed ADL, ASE, and ASH neurons elicits avoidance response in *Caenorhabditis elegans*. *Neuroreport* 10: 753-757.
- Savage, C., P. Das, A. L. Finelli, S. R. Townsend, C. Y. Sun et al., 1996. *Caenorhabditis elegans* genes *sma-2*, *sma-3*, and *sma-4* define a conserved family of transforming growth factor  $\beta$  pathway components. *Proc Natl Acad Sci U S A* 93: 790-794.
- Schouest, K., A. Zitova, C. Spillane and D. Papkovsky, 2009. Toxicological assessment of chemicals using *Caenorhabditis elegans* and optical oxygen respirometry. *Environ Toxicol Chem* 28: 791-799.
- Schulenburg, H., C. L. Kurz and J. J. Ewbank, 2004. Evolution of the innate immune system: the worm perspective. *Immunol Rev* 198: 36-58.

- Schultz, R. D., E. E. Bennett, E. A. Ellis and T. L. Gumienny, 2014. Regulation of extracellular matrix organization by BMP signaling in *Caenorhabditis elegans*. PLoS One 9: e101929.
- Sekelsky, J. J., S. J. Newfeld, L. A. Raftery, E. H. Chartoff and W. M. Gelbart, 1995. Genetic characterization and cloning of mothers against *Dpp*, a gene required for decapentaplegic function in *Drosophila melanogaster*. Genetics 139: 1347-1358.
- Shi, M., J. Zhu, R. Wang, X. Chen, L. Mi et al., 2011. Latent TGF- $\beta$  structure and activation. Nature 474: 343-349.
- Shi, Y., and J. Massague, 2003. Mechanisms of TGF- $\beta$  signaling from cell membrane to the nucleus. Cell 113: 685-700.
- Simmons S. P., S. J. C., 1997. Measuring emotional intelligence. Summit Publishing Group, New York.
- Solis, G. M., and M. Petrascheck, 2011. Measuring *Caenorhabditis elegans* life span in 96 well microtiter plates. J Vis Exp.
- Souchelnytskyi, S., K. Tamaki, U. Engstrom, C. Wernstedt, P. ten Dijke et al., 1997. Phosphorylation of Ser465 and Ser467 in the C terminus of Smad2 mediates interaction with Smad4 and is required for transforming growth factor- $\beta$  signaling. J Biol Chem 272: 28107-28115.

- Strick, R., P. L. Strissel, K. Gavrilov and R. Levi-Setti, 2001. Cation-chromatin binding as shown by ion microscopy is essential for the structural integrity of chromosomes. *J Cell Biol* 155: 899-910.
- Sulston, J. E., and H. R. Horvitz, 1977. Post-embryonic cell lineages of the nematode, *Caenorhabditis elegans*. *Dev Biol* 56: 110-156.
- Sumakovic, M., J. Hegermann, L. Luo, S. J. Husson, K. Schwarze et al., 2009. UNC-108/RAB-2 and its effector RIC-19 are involved in dense core vesicle maturation in *Caenorhabditis elegans*. *J Cell Biol* 186: 897-914.
- Suzuki, Y., M. D. Yandell, P. J. Roy, S. Krishna, C. Savage-Dunn et al., 1999. A BMP homolog acts as a dose-dependent regulator of body size and male tail patterning in *Caenorhabditis elegans*. *Development* 126: 241-250.
- Tennant, C., 1999. Life stress, social support and coronary heart disease. *Aust N Z J Psychiatry* 33: 636-641.
- Tian, Y., Z. Li, W. Hu, H. Ren, E. Tian et al., 2010. *C. elegans* screen identifies autophagy genes specific to multicellular organisms. *Cell* 141: 1042-1055.
- Tisdale, E. J., J. R. Bourne, R. Khosravi-Far, C. J. Der and W. E. Balch, 1992. GTP-binding mutants of Rab1 and Rab2 are potent inhibitors of vesicular transport from the endoplasmic reticulum to the Golgi complex. *J Cell Biol* 119: 749-761.

- Walshe, T. E., N. G. dela Paz and P. A. D'Amore, 2013. The role of shear-induced transforming growth factor- $\beta$  signaling in the endothelium. *Arterioscler Thromb Vasc Biol* 33: 2608-2617.
- Wang, J., R. Tokarz and C. Savage-Dunn, 2002. The expression of TGF $\beta$  signal transducers in the hypodermis regulates body size in *C. elegans*. *Development* 129: 4989-4998.
- Warnhoff, K., J. T. Murphy, S. Kumar, D. L. Schneider, M. Peterson et al., 2014. The DAF-16 FOXO transcription factor regulates *nac-1* to modulate stress resistance in *Caenorhabditis elegans*, linking insulin/IGF-1 signaling to protein N-terminal acetylation. *PLoS Genet* 10: e1004703.
- Williams, P. L., and D. B. Dusenbery, 1988. Using the nematode *Caenorhabditis elegans* to predict mammalian acute lethality to metallic salts. *Toxicol Ind Health* 4: 469-478.
- Wu, M. Y., and C. S. Hill, 2009. TGF-beta superfamily signaling in embryonic development and homeostasis. *Dev Cell* 16: 329-343.
- Wu, X., Y. Guan, J. Yan, M. Liu, Y. Yin et al., 2015. ShenKang injection suppresses kidney fibrosis and oxidative stress via transforming growth factor- $\beta$ /Smad3 signalling pathway *in vivo* and *in vitro*. *J Pharm Pharmacol* 67: 1054-1065.



- Yoshida, S., K. Morita, M. Mochii and N. Ueno, 2001. Hypodermal expression of *Caenorhabditis elegans* TGF- $\beta$  type I receptor SMA-6 is essential for the growth and maintenance of body length. *Dev Biol* 240: 32-45.
- Yoshimura, A., Y. Wakabayashi and T. Mori, 2010. Cellular and molecular basis for the regulation of inflammation by TGF- $\beta$ . *J Biochem* 147: 781-792.
- Zugasti, O., and J. J. Ewbank, 2009. Neuroimmune regulation of antimicrobial peptide expression by a noncanonical TGF- $\beta$  signaling pathway in *Caenorhabditis elegans* epidermis. *Nat Immunol* 10: 249-256.

## APPENDIX A

ELUCIDATING THE ROLE OF INSULIN SIGNALING IN DYF-7 RESPONSES IN *C.*

*ELEGANS*

## Introduction

Sensing environmental cues is an essential factor in stress-response. There are specific sensory neurons in *C. elegans* that sense and interpret environmental cues that signal survival and reproductive potential, including nutrient availability, temperature, and population density. The tectorin-like ZP-domain protein DYF-7 helps anchor the dendritic tips of those specific sensory neurons, amphids and phasmids, to the basement membrane as the cells migrate during embryogenesis and are expressed in the same cells as the insulin signaling ligand, DAF-2 (Parasuraman 2011). Perhaps because animals cannot sense favorable environments, some *dyf-7* mutants in a population will remain arrested in the first larval stage, L1 (at 20°C) (Heiman and Shaham 2009).

Insulin signaling pathway mutants also affect the L1 arrest/progression decision. *daf-2* mutants exhibit L1 arrest in 20% of the population and dauers in 45% of the populations at 27°C (Dillin *et al.* 2002). In unfavorable conditions (low food supply, high temperature, and/or high population), a downstream member of the insulin signaling pathway, DAF-16, is crucial to stopping development throughout the animal during stress (Kaplan *et al.* 2015). *daf-16* mutants exhibit L1 arrest defective and dauer defective animal populations (Lee *et al.* 2001). Functional loss of the sole insulin receptor in *C. elegans*, DAF-2, which is expressed in the environment sensing cells that require DYF-7 for proper anchoring, increases the percentage of animals that arrest in the L1 stage at 25 to 27°C (Heiman and Shaham 2009). DAF-2 negatively regulates DAF-16, and loss of DAF-16 function prevents animals from arresting at L1 at high temperature (Warnhoff *et*

*al.* 2014). Clarifying the cross-talk between environment sensing and insulin signaling will help understand the organismal stress response to environmental stressors.

## Materials and Methods

### Strains and maintenance

*C. elegans* strains that were used in these studies are derived from the wild-type variety Bristol strain N2 and cultured on nematode growth media (NGM) plates as previously described (Brenner 1974). All strains were cultured on *E. coli* strain OP50 at 20°C, except where noted. Strains used include: TLG552 *rrf-3(pk1426)* II and SP1196 *dyf-7(m539)* X.

### L1 arrest Assay

L1 arrest temperature assays were conducted as previously described (Strick *et al.* 2001). Briefly, animals used in experiments requiring gene-specific RNAi were grown continuously and for multiple generations on bacteria expressing gene-specific (*daf-2* and *daf-16*) or negative control (pseudogene C06C3.5) dsRNA. Animals were then staged at embryo stage by placing RNAi-treated gravid adults on test plates seeded with bacteria expressing gene-specific dsRNA, where they laid embryos at 20°C for 5 hours before being removed. The embryos were then incubated at the 27°C test temperature for 44 hours, the time required for wild-type animals to enter late larval or early adult stages before any F1 embryos are laid. After the incubation period, the developmental stage of each animal was scored. Assays were independently performed three times, with at least 50 animals total per genotype. Reliability analysis and Mann-Whitney U test were used for statistical analysis.

## Results and Discussion

### *dyf-7(-)* L1 arrest and dauer entry defects do not require functional insulin signaling

To test if the L1 arrest phenotype displayed by *dyf-7* mutant animals requires a functional insulin signaling pathway, we observed the ability of *dyf-7* mutant animals to exit L1 in a replete but stressfully warm (27°C) environment in *daf-2* or *daf-16* RNAi conditions. *daf-2* mutants exhibit L1 arrest in 20% of the population and dauers in 45% of the populations at 27°C (Dillin *et al.* 2002). *daf-16* mutants exhibit L1 arrest defective and dauer defective animal populations (Lee *et al.* 2001). RNAi against *daf-2* or *daf-16* in *rrf-3(pk1426)* RNAi-sensitized animals phenocopied their mutant phenotypes. *daf-2(RNAi)* increased the population of animals arrested at L1 (when control populations have all progressed to dauer stage or adulthood proving that our RNAi works efficiently (see Figure A.1). Loss of *daf-2* in the *rrf-3(pk1426)* background caused a significantly lower ( $p < 0.05$ ) percentage of animals in the population that remained arrested in L1 (5.9%) compared to *dyf-7(m539); rrf-3(pk1426)* (94.9%) (see Figure A.1). *daf-16 (RNAi)* populations at 27°C had no dauers, and also had reduced population arrested at L1 (0.9%), consistent with DAF-16's role in promoting dauer formation. However, loss of *daf-16* in the *dyf-7(m539); rrf-3(pk1426)* background had no significant effect on the percentage of animals in the population that remained arrested in L1 (93.8%) compared to control. DYF-7 function does not require a functional DAF-2 pathway, indicating that the developmental decisions associated with loss of *dyf-7* occur independent of the insulin signaling pathway. Hence, environmental sensing by downstream response of the

DAF-2/DAF-16 pathway is not required for DYF-7 responses. This knowledge helps us better understand the molecular basis of organismal responses to stress.

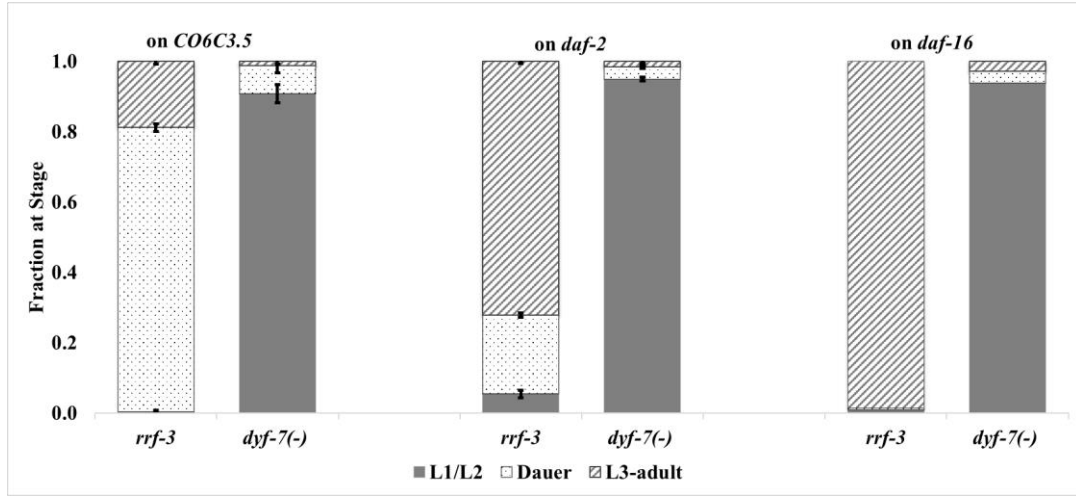


Figure A.1. DAF-2 and DAF-16 do not affect DYF-7 function. Assays performed with *rrf-3*, and *dyf-7(-)* strains on *daf-2* and *daf-16* RNAi with *CO6C3.5* as control. Values are averages from at least 3 independent experiments ( $n > 50$  animals) for each condition. Error bars reflect the standard deviation (SD).